Electronic Supplementary Material (ESI) for Organic & Biomolecular Chemistry.

Development of Photoswitchable Inhibitors for β-Galactosidase

Karin Rustler,[a] Matthias J. Mickert,[b] Julian Nazet,[c] Rainer Merkl,[c] Hans H. Gorris,[b] and Burkhard König*[a]

[a] InstituteP of Organic Chemistry, University of Regensburg, 93053 Regensburg, Germany
E-mail: burkhard.koenig@ur.de

[b] Institute of Analytical Chemistry, Chemo- and Biosensors, University of Regensburg, 93053 Regensburg, Germany

[c] Institute of Biophysics and Physical Biochemistry, University of Regensburg, 93053 Regensburg, Germany

Supporting Information

Table of Contents

Experimental procedures

Chemistry

Commercial reagents and starting materials were purchased from the commercial suppliers abcr, Acros Organics, Alfa-Aesar, Fisher Scientific, Merck, Sigma Aldrich, TCI, or VWR and used without any further purification. Solvents were used in p.a. quality and dried according to common procedures, if necessary. Dry nitrogen was used as an inert gas atmosphere. Flash column chromatography was performed using Sigma Aldrich MN silica gel 60 M (40-63 µm, 230-400 mesh) for normal phase chromatography. Reaction monitoring *via* thin layer chromatography was performed on alumina plates coated with silica gel (Merck silica gel 60 F254, layer thickness 0.2 mm). Melting points were determined using a Stanford Research System OptiMelt MPA 100 and are uncorrected. NMR spectra were measured on a Bruker Avance 300 (^{1}H 300.13 MHz, ^{13}C 75.48 MHz), Bruker Avance III HD 400 (^{1}H 400.13 MHz, ^{13}C 100.61 MHz), Bruker Avance III HD 600 (^{1}H 600.25 MHz, ^{13}C 150.95 MHz) and Bruker Avance III 600 (^{1}H 600.25 MHz, ^{1}3C 150.95 MHz). The spectra are referenced against the NMR-solvent (DMSO-d_6: δ_H = 2.50 ppm, δ_C = 39.52 ppm; $CDCl_3$- *d*: δ_H = 7.26 ppm, δ_C = 77.16 ppm) and chemical shifts δ are reported in ppm. Resonance multiplicity is abbreviated as: s (singlet), d (doublet), t (triplet) and m (multiplet). Carbon NMR signals are assigned using DEPT 135 and ^{1}H-^{13}C HSQC spectra with (+) for primary/tertiary, (-) for secondary, and (q) for quaternary carbons. Mass spectra were recorded on a Finnigan MAT-SSQ 710 A, ThermoQuest Finnigan TSQ 7000, Agilent Q-TOF 6540 UHD, or a Jeol AccuTOF GCX instrument. UV/Vis absorption spectroscopy was performed in 10 mm quartz cuvettes using an Agilent 8543, Agilent Cary 100, or Agilent Varian Cary 50 spectrometer. Analytical HPLC measurements were performed using an Agilent 1220 Infinity LC (column: Phenomenex Luna 3 µm C18(2) 100 A, 150 x 2.00 mm; flow 0.3 mL min^{-1} at 20 °C or 30 °C; solvent A: MilliQ water with 0.05 wt% TFA; solvent B: MeCN). The ratios at the PSSs were determined *via* analytical HPLC at 20 °C at the isosbestic points or *via* NMR spectroscopy. An Agilent 1260 system (column: Phenomenex Luna 10 µm C18(2) 100 A, 250 x 21.2 mm; flow: 22 mL min^{-1}; solvent A: MilliQ water; solvent B: MeCN) was used for preparative HPLC purification. Light sources for irradiation: λ = 365 nm (Seoul Viosys CUN6GB1A, 1000 mA, 1.4 W), λ = 385 nm (Seoul Viosys CUN8GF1A, 1000 mA, 1.6 W), λ = 455 nm (Osram OSLON SSL 80 LD-CQ7P-1U3U, 1000 mA, 0.45 W), λ = 470 nm (Osram OSLON SSL 80 LBCP7P-GYHY, 1000 mA, 50.4 lm), and λ = 505 nm (Osram OSLON SSL 80 LVCK7P-JYKZ, 800 mA, 163 lm). The power of the light is given based on the specifications supplied by the company when the LEDs were purchased. All tested final compounds possess a purity ≥93% determined by HPLC measurements at 30 °C with detection at 220 nm or 254 nm, respectively. All biological investigations were performed in the group of PD Dr. Hans H. Gorris by Matthias J. Mickert (University of Regensburg). Docking analysis was performed by the group of Prof. Dr. Rainer Merkl by Julian Nazet (University of Regensburg).

Compounds **8**,[1] **9**,[2] **10**,[2] **24**[3] were prepared according to previously reported procedures.

(2*R*,3*R*,4*S*,5*R*,6*R*)-2-amino-6-(hydroxymethyl)tetrahydro-2*H*-pyran-3,4,5-triol (2)

Galactosylamine **2** was synthesized via an adapted literature procedure.[4] Therefore, D-Galactose (1.0 g, 5.5 mmol, 1.0 eq) was dissolved in a solution of ammonia in methanol (40 mL, 7.0 M, 0.28 mol, 50 eq) and stirred at room temperature for 48 hours until a colourless solid precipitated. The product was filtered, washed with cold methanol (2 x 5 mL) and diethyl ether (2 x 5 mL) and dried *in vacuo* to afford **2** in its β-pyranose form in 63% yield (3.5 mmol, 0.62 g). The measured NMR spectra was in accordance with the literature reported spectra.

4-((*E*)-phenyldiazenyl)-*N*-((2*R*,3*R*,4*S*,5*R*,6*R*)-3,4,5-trihydroxy-6-(hydroxymethyl)tetrahydro-2*H*-pyran-2-yl)benzamide (4)

To a stirred solution of galactosylamine **2** (0.17 g, 0.94 mmol, 2.3 eq) and potassium carbonate (56 mg, 0.41 mmol, 1.0 eq) in water (2 mL) was added a solution of phenylazobenzoylchloride **3** (0.25 g, 1.0 mmol, 2.4 eq) in acetone (8 mL) and stirred at room temperature for 14 hours.[5] Thin layer chromatography indicated complete consumption of the phenylazobenzoylchloride. Purification by column chromatography (CH_2Cl_2 + 5% MeOH) afforded the desired product which was further purified by preparative HPLC (column: Phenomenex Luna 10 µm C18(2) 100 Å, gradient 0-16 min 75:25 -66:34, t_R = 12.5 min) to afford the product as orange solid in good yield (0.30 g, 0.77 mmol, 82%). m.p. 189 °C. ^{1}H-NMR (400 MHz, DMSO-*d*$_6$): δ = 8.56 (d, *J* = 8.7 Hz, 1H), 8.10 (d, *J* = 8.3 Hz, 2H), 7.99 – 7.91 (m, 4H), 7.65 – 7.58 (m, 3H), 5.68 (dd, *J* = 8.7, 5.4 Hz, 1H), 5.02 – 4.92 (m, 1H), 4.69 – 4.50 (m, 2H), 4.40 (d, *J* = 4.5 Hz, 1H), 4.01 – 3.91 (m, 1H), 3.87 (s, 1H), 3.78 – 3.73 (m, 1H), 3.71 (t, *J* = 6.2 Hz, 1H), 3.57 – 3.50 (m, 1H), 3.44 – 3.38 (m, 1H). ^{13}C-NMR (101 MHz, DMSO-*d*$_6$): δ =167.1 (q), 153.4 (q), 151.9 (q), 136.8 (q), 132.1 (+), 129.6 (+), 129.2 (+), 122.8 (+), 122.2 (+), 77.2 (+), 72.3 (+), 69.0 (+), 68.5 (+), 67.0 (+), 60.4 (-). HRMS (ESI) calcd. for ($C_{19}H_{22}N_3O_6$+) $[M+H]^+$: m/z = 388.1503; found 388.1502.

(2*R*,3*R*,4*S*,5*R*,6*R*)-2-(hydroxymethyl)-6-((4-((*E*)-phenyldiazenyl)phenyl)amino)tetrahydro-2*H*-pyran-3,4,5-triol (6)

Compound **6** was synthesized according to an adapted literature procedure.[6] *Para* aminoazobenzene (1.0 g, 5.2 mmol, 1.0 eq) was added to a solution of β-D-galactose (0.90 g, 5.0 mmol, 1.0 eq) in a mixture of EtOH and water (20 mL, 3:1). The reaction was heated to reflux for four hours and at room temperature for additional 16 hours. The mixture was extracted with ethyl acetate (3x 20 mL). The organic phase was dried over $MgSO_4$ and the solvent was evaporated. The product was purified by column chromatography (CH_2Cl_2 + 5% MeOH) and preparative HPLC (column: Phenomenex Luna 10 µm C18(2) 100 Å, gradient 0-12 min 10:90 -37:63, t_R = 10.0 min) to yield the desired product in good yield as orange solid (1.40 g, 3.90 mmol, 78%). m.p. 131 °C. ^{1}H-NMR (400 MHz, DMSO-*d*$_6$): δ = 7.81 – 7.70 (m, 4H), 7.57 – 7.47 (m, 2H), 7.45 – 7.39 (m, 1H), 7.17 (d, *J* = 7.7 Hz, 1H), 6.90 – 6.82 (m, 2H), 4.81 (t, *J* = 5.2 Hz, 2H), 4.60 (t, *J* = 5.1 Hz, 1H), 4.54 – 4.41 (m, 2H), 3.76 (t, *J* = 3.8 Hz, 1H), 3.62 – 3.51 (m, 3H), 3.51 – 3.41 (m, 2H). ^{13}C-NMR (101 MHz, DMSO-*d*$_6$): δ = 152.8 (q), 151.5 (q), 144.2 (q), 130.2 (+), 129.7 (+), 125.2 (+), 122.3 (+), 113.5 (+), 85.0 (+), 76.3 (+), 74.8 (+), 70.5 (+), 68.9 (+), 61.0 (-). HRMS (ESI) calcd. for ($C_{18}H_{22}N_3O_5$+) $[M+H]^+$: m/z = 360.1554; found 360.1558.

General procedure for the synthesis of pentaacetylated-thiogalactoside nitrobenzene precursors 11-16:

The compounds were synthesized following an adapted literature procedure.[7] To a solution of β-D-thiogalactoside **10** (2.0 g, 5.5 mmol, 1.0 eq) in CH_3CN (20 mL) was added the respective bromo-substituted nitrobenzene (6.0 mmol, 1.1 eq) and triethylamine (0.80 mL, 6.0 mmol, 1.1 eq) and stirred at room temperature until TLC indicated consumption of the starting material. The solvent was evaporated and the mixture separated between water and ethyl acetate. The organic phase was dried ($MgSO_4$), the solvent evaporated, and the residue purified by flash column chromatography (PE/EA 1/1) to afford the desired products in moderate to good yields.

(2*R*,3*S*,4*S*,5*R*,6*S*)-2-(acetoxymethyl)-6-((2-nitrophenethyl)thio)tetrahydro-2*H*-pyran-3,4,5-triyl triacetate (11)

White foam: 76% yield; ^{1}H-NMR (300 MHz, $CDCl_3$-*d*): δ = 7.95 (dd, *J* = 8.5, 1.4 Hz, 1H), 7.60 – 7.49 (m, 1H), 7.45 – 7.32 (m, 2H), 5.44 (dd, *J* = 3.4, 1.1 Hz, 1H), 5.25 (t, *J* = 10.0 Hz, 1H), 5.06 (dd, *J* = 10.0, 3.4 Hz, 1H), 4.58 (d, *J* = 9.9 Hz, 1H), 4.13 (dd, 2H), 4.04 – 3.92 (m, 1H), 3.33 – 3.12 (m, 2H), 3.11 – 2.95 (m, 1H), 2.98 – 2.77 (m, 1H), 2.15 (s, 3H), 2.05 (s, 3H), 1.99 (s, 3H), 1.97 (s, 3H). ^{13}C-NMR (75 MHz, $CDCl_3$-*d*): δ = 170.5 (q), 170.4 (q), 170.1 (q), 169.7 (q), 149.2 (q), 135.1 (q), 133.4 (+), 132.7 (+), 127.9 (+), 125.1 (+),

84.5 (+), 74.7 (+), 72.0 (+), 67.4 (+), 67.3 (+), 61.6 (-), 34.7 (-), 31.0 (-), 20.9 (+), 20.8 (+), 20.8 (+), 20.7 (+). HRMS (ESI) calcd. for ($C_{22}H_{27}NO_{11}SNa^+$) $[M+Na]^+$: m/z = 536.1197; found 536.1197.

(2*R*,3*S*,4*S*,5*R*,6*S*)-2-(acetoxymethyl)-6-((4-nitrophenethyl)thio)tetrahydro-2*H*-pyran-3,4,5-triyl triacetate (12)

White foam: 82% yield; ^{1}H-NMR (400 MHz, $CDCl_3$-*d*): δ = 8.03 (d, *J* = 8.7 Hz, 2H), 7.29 (d, *J* = 8.7 Hz, 2H), 5.34 (d, *J* = 3.4, 1.1 Hz, 1H), 5.15 (t, *J* = 10.0 Hz, 1H), 4.98 (dd, *J* = 10.0, 3.4 Hz, 1H), 4.45 (d, *J* = 9.9 Hz, 1H), 4.06 – 3.98 (m, 2H), 3.91 (t, 1H), 3.00 – 2.90 (m, 3H), 2.90 – 2.81 (m, 1H), 2.04 (s, 3H), 1.93 (s, 3H), 1.91 (s, 3H), 1.87 (s, 3H). ^{13}C-NMR (101 MHz, $CDCl_3$-*d*): δ = 170.2 (q), 170.0 (q), 169.9 (q), 169.5 (q), 147.8 (q), 146.6 (q), 129.5 (+), 123.6 (+), 83.8 (+), 74.5 (+), 71.7 (+), 67.3 (+), 66.9 (+), 61.6 (-), 35.9 (-), 30.4 (-), 20.7 (+), 20.6 (+), 20.6 (+), 20.5 (+). HRMS (ESI) calcd. for ($C_{22}H_{27}NO_{11}SNa^+$) $[M+Na]^+$: m/z = 536.1197; found 536.1196.

(2*R*,3*S*,4*S*,5*R*,6*S*)-2-(acetoxymethyl)-6-((2-nitrobenzyl)thio)tetrahydro-2*H*-pyran-3,4,5-triyl triacetate (13)

White viscous solid: 72% yield; ^{1}H-NMR (300 MHz, $CDCl_3$-*d*): δ = 7.92 (dd, *J* = 8.1, 1.5 Hz, 1H), 7.57 – 7.47 (m, 1H), 7.46 – 7.35 (m, 2H), 5.35 (dd, *J* = 3.3, 1.2 Hz, 1H), 5.17 (t, *J* = 10.0 Hz, 1H), 4.92 (dd, *J* = 10.0, 3.4 Hz, 1H), 4.30 (d, *J* = 10.0 Hz, 1H), 4.19 (s, 2H), 4.04 – 3.98 (m, 2H), 3.79 (td, *J* = 6.6, 1.2 Hz, 1H), 2.11 (s, 3H), 2.01 (s, 3H), 1.96 (s, 3H), 1.91 (s, 3H). ^{13}C-NMR (75 MHz, $CDCl_3$-*d*): δ = 170.4 (q), 170.2 (q), 170.0 (q), 169.6 (q), 148.7 (q), 133.5 (q), 133.0 (+), 132.2 (+), 128.6 (+), 125.3 (+), 83.2 (+), 74.5 (+), 71.7 (+), 67.2 (+), 67.0 (+), 61.4 (-), 31.3 (-), 20.7 (+), 20.7 (+), 20.7 (+), 20.6 (+). HRMS (ESI) calcd. for ($C_{21}H_{25}NO_{11}SNa^+$) $[M+Na]^+$: m/z = 522.1041; found 522.1044.

(2*R*,3*S*,4*S*,5*R*,6*S*)-2-(acetoxymethyl)-6-((4-nitrobenzyl)thio)tetrahydro-2*H*-pyran-3,4,5-triyl triacetate (14)

White foam: 44% yield; ^{1}H-NMR (300 MHz, $CDCl_3$-*d*): δ = 8.19 – 8.13 (m, 2H), 7.51 – 7.45 (m, 2H), 5.41 (dd, *J* = 3.4, 1.2 Hz, 1H), 5.28 (t, *J* = 10.0 Hz, 1H), 4.99 (dd, *J* = 10.0, 3.4 Hz, 1H), 4.32 (d, *J* = 9.9 Hz, 1H), 4.12 – 4.00 (m, 3H), 3.95 – 3.84 (m, 2H), 2.15 (s, 3H), 2.05 (s, 3H), 2.04 (s, 3H), 1.96 (s, 3H). ^{13}C-NMR (75 MHz, $CDCl_3$-*d*): δ = 170.3 (q), 170.1 (q), 170.0 (q), 169.7 (q), 147.2 (q), 144.9 (q), 130.0 (+), 123.8 (+), 82.4 (+), 74.7 (+), 71.6 (+), 67.2 (+), 66.9 (+), 61.5 (-), 32.8 (-), 20.8 (+), 20.7 (+), 20.7 (+), 20.6 (+). HRMS (ESI) calcd. for ($C_{21}H_{25}NO_{11}SNa^+$) $[M+Na]^+$: m/z = 522.1041; found 522.1045.

(2*R*,3*S*,4*S*,5*R*,6*S*)-2-(acetoxymethyl)-6-((2-nitrophenyl)thio)tetrahydro-2*H*-pyran-3,4,5-triyl triacetate (15)

White viscous solid: 61% yield; ^{1}H-NMR (300 MHz, $CDCl_3$-*d*): δ = 8.09 (dd, *J* = 8.1, 1.5 Hz, 1H), 7.82 (dd, *J* = 8.1, 1.3 Hz, 1H), 7.57 (ddd, *J* = 8.1, 7.3, 1.5 Hz, 1H), 7.40 (ddd, *J* = 8.4, 7.3, 1.3 Hz, 1H), 5.48 (dd, *J* = 3.4, 1.0 Hz, 1H), 5.35 (t, *J* = 10.0 Hz, 1H), 5.10 (dd, *J* = 9.9, 3.3 Hz, 1H), 4.85 (d, *J* = 10.0 Hz, 1H), 4.22 – 4.10 (m, 2H), 4.08 – 4.02 (m, 1H), 2.17 (s, 3H), 2.06 (s, 3H), 2.03 (s, 3H), 1.98 (s, 3H). ^{13}C-NMR (75 MHz, $CDCl_3$-*d*): δ = 170.3 (q), 170.1 (q), 170.0 (q), 169.3 (q), 148.4 (q), 133.2 (+), 132.5 (q), 130.2 (+), 127.1 (+), 125.5(+), 84.6 (+), 74.7 (+), 71.9 (+), 67.1 (+), 66.4 (+), 61.8 (-), 20.7 (+), 20.7 (+), 20.7 (+), 20.6 (+). HRMS (ESI) calcd. for ($C_{20}H_{23}NO_{11}SNa^+$) $[M+Na]^+$: m/z = 508.0884; found 508.0882.

(2*R*,3*S*,4*S*,5*R*,6*S*)-2-(acetoxymethyl)-6-((4-nitrophenyl)thio)tetrahydro-2*H*-pyran-3,4,5-triyl triacetate (16)

White foam: 68% yield; ^{1}H-NMR (400 MHz, DMSO-d_6): δ = 8.19 (d, *J* = 8.9 Hz, 2H), 7.66 (d, *J* = 9.0 Hz, 2H), 5.56 (d, *J* = 10.0 Hz, 1H), 5.42 – 5.38 (m, 1H), 5.31 (dd, *J* = 9.9, 3.4 Hz, 1H), 5.13 (t, *J* = 9.9 Hz, 1H), 4.47 – 4.40 (m, 1H), 4.14 – 4.01 (m, 2H), 2.15 (s, 3H), 2.05 (s, 3H), 2.01 (s, 3H), 1.94 (s, 3H). ^{13}C-NMR (101 MHz, DMSO-d_6): δ =170.4 (q), 170.3 (q), 169.9 (q), 169.8 (q), 146.3 (q), 143.7 (q), 129.2 (+), 124.4

(+), 82.6 (+), 74.3 (+), 71.3 (+), 68.0 (+), 67.0 (+), 62.2 (-), 21.0 (+), 20.9 (+), 20.9 (+), 20.8 (+). HRMS (ESI) calcd. for ($C_{20}H_{23}NO_{11}SNa^+$) $[M+Na]^+$: m/z = 508.0884; found 508.0882.

General procedure for reduction to pentaacetylated-thiogalactoside aminobenzenes 17-22:

For the reduction of the nitro-groups of the pentaacetylated-thiogalactoside nitrobenzenes **17**-**22** (4.0 mmol, 1.0 eq) were dissolved in a mixture of EtOH (60 mL) and CH_2Cl_2 (20 mL). Tin(II)chloride dihydrate (3.6 g, 16.0 mmol, 4.0 eq) was added and the mixture heated to reflux at 80 °C for four to six hours until TLC indicated complete consumption of the starting material and ninhydrin stain positive amine formation. The solvent was removed and the residue portioned between EtOAc (200 mL) and $NaHCO_3$. The organic phase was dried over $MgSO_4$, the solvent was evaporated and the crude product directly used in the next step without further purification.[8]

General preparation for the formation of PETG-based azobenzene derivatives 34-42:

The pentaacetylated-thiogalactoside aminobenzenes **17**-**22** (1.0 eq) and the respective nitrosobenzene (1.0 eq) were dissolved in a mixture of acetic acid and CH_2Cl_2 (1:1) and stirred at room temperature for 16 hours. The solvent was evaporated and the product purified by flash column chromatography (CH_2Cl_2). Deprotection of the sugar-moiety was achieved by dissolving the protected compound in methanol and addition of potassium carbonate (0.50 eq).[9] The crude products were purified by flash column chromatography (CH_2Cl_2 + 5% MeOH) and preparative HPLC (column: Phenomenex Luna 10 µm C18(2) 100 Å) to afford the desired products in moderate to good yields.

(2*R*,3*R*,4*S*,5*R*,6*S*)-2-(hydroxymethyl)-6-((2-((*E*)-phenyldiazenyl)phenethyl)thio)tetrahydro-2*H*-pyran-3,4,5-triol (34)

Orange solid (51%). Gradient 0-20 min 10:90 -98:2, t_R = 11.7 min. m.p. 139 °C. ^{1}H NMR (400 MHz, DMSO-d_6) δ = 7.94 – 7.85 (m, 2H), 7.65 – 7.54 (m, 4H), 7.53 – 7.44 (m, 2H), 7.41 – 7.33 (m, 1H), 4.92 (d, *J* = 5.7 Hz, 1H), 4.76 (d, *J* = 5.6 Hz, 1H), 4.54 (t, *J* = 5.6 Hz, 1H), 4.38 (d, *J* = 4.4 Hz, 1H), 4.25 (d, *J* = 9.4 Hz, 1H), 3.67 (t, *J* = 3.9 Hz, 1H), 3.52 – 3.32 (m, 6H), 3.29 – 3.19 (m, 1H), 3.00 – 2.83 (m, 2H). ^{13}C NMR (101 MHz, DMSO) δ = 152.8 (+), 149.9 (+), 141.0 (+), 132.1 (+), 131.9 (+), 131.6 (+), 130.0 (+), 127.8 (+), 123.1 (+), 115.5 (+), 86.3 (+), 79.6 (+), 75.2 (+), 70.3 (+), 68.8 (+), 61.0 (-), 32.4 (-), 31.7 (-).HRMS (ESI) calcd. for ($C_{20}H_{25}N_2O_5S^+$) $[M+H]^+$: m/z = 405.1479; found 405.1482.

(2*R*,3*R*,4*S*,5*R*,6*S*)-2-(hydroxymethyl)-6-((4-((*E*)-phenyldiazenyl)phenethyl)thio)tetrahydro-2*H*-pyran-3,4,5-triol (35)

Orange solid (62%). Gradient 0-11 min 28:72 - 70:30, t_R = 8.57 min. m.p.: 162 °C. ^{1}H NMR (400 MHz, DMSO-d_6) δ = 7.90 – 7.86 (m, 2H), 7.85 – 7.81 (m, 2H), 7.62 – 7.53 (m, 3H), 7.51 – 7.45 (m, 2H), 4.97 (d, *J* = 5.7 Hz, 1H), 4.80 (d, *J* = 5.6 Hz, 1H), 4.60 (t, *J* = 5.6 Hz, 1H), 4.42 (d, *J* = 4.4 Hz, 1H), 4.29 (d, *J* = 9.4 Hz, 1H), 3.70 (t, *J* = 3.9 Hz, 1H), 3.52 (t, *J* = 5.6 Hz, 2H), 3.43 – 3.36 (m, 2H), 3.32 – 3.27 (m, 1H), 3.01 – 2.92 (m, 3H), 2.92 – 2.82 (m, 1H). ^{13}C NMR (101 MHz, DMSO) δ 152.4 (-), 150.9 (-), 145.4 (-), 131.8 (+), 130.1 (+), 129.9 (+), 123.0 (+), 122.9 (+), 86.1 (+), 79.7 (+), 75.2 (+), 70.2 (+), 69.0 (+), 61.2 (-), 36.3 (-), 30.7 (-).HRMS (ESI) calcd. for ($C_{20}H_{24}N_2O_5SNa^+$) $[M+Na]^+$: m/z = 427.1300; found 427.1298.

(2*R*,3*S*,4*S*,5*R*,6*S*)-2-(acetoxymethyl)-6-((2-((*E*)-(4-(tert-butyl)phenyl)diazenyl)phenethyl)thio)tetrahydro-2*H*-pyran-3,4,5-triyl triacetate (36)

Orange solid (19%). Gradient 0-20 min 10:90 - 98:2, t_R = 15.7 min. m.p. 109 °C. ^{1}H NMR (400 MHz, DMSO-d_6) δ = 7.83 (d, *J* = 8.6 Hz, 2H), 7.62 (d, *J* = 8.5 Hz, 2H), 7.59 – 7.56 (m, 1H), 7.51 – 7.44 (m, 2H), 7.38 – 7.34 (m, 1H), 5.34 – 4.29 (m, 5H), 4.24 (d, *J* = 9.4 Hz, 1H), 3.67 (d, *J* = 3.1 Hz, 1H), 3.52 – 3.37 (m, 4H), 3.30 – 3.18 (m, 2H), 2.94 – 2.85 (m, 2H), 1.33 (s, 9H). ^{13}C NMR (101 MHz, DMSO) δ = 154.5 (q), 150.4 (q), 149.5 (q), 140.3 (q), 131.3 (+), 131.1 (+), 127.3 (+), 126.3 (+), 122.4 (+), 115.0 (+), 85.9 (+),

79.1 (+), 74.7 (+), 69.9 (+), 68.3 (+), 60.5 (-), 34.8 (q), 32.0 (-), 31.3 (-), 31.0 (+). HRMS (ESI) calcd. for ($C_{24}H_{32}N_2O_5SNa^+$) $[M+Na]^+$: m/z = 483.1924; found 483.192.4

(2*R*,3*R*,4*S*,5*R*,6*S*)-2-(hydroxymethyl)-6-((2-((*E*)-phenyldiazenyl)benzyl)thio)tetrahydro-2*H*-pyran-3,4,5-triol (37)

Orange solid (22%). Gradient 0-20 min 10:90 - 98:2, t_R = 11.1 min. m.p. 179 °C. ^{1}H NMR (400 MHz, DMSO-d_6) δ = 7.96 – 7.91 (m, 2H), 7.65 – 7.55 (m, 5H), 7.52 – 7.47 (m, 1H), 7.43 – 7.39 (m, 1H), 4.90 (d, *J* = 5.9 Hz, 1H), 4.76 (d, *J* = 5.6 Hz, 1H), 4.66 (t, *J* = 5.6 Hz, 1H), 4.44 – 4.38 (m, 2H), 4.33 (d, *J* = 12.6 Hz, 1H), 4.15 (d, *J* = 9.5 Hz, 1H), 3.68 (t, *J* = 4.0 Hz, 1H), 3.54 (t, *J* = 5.8 Hz, 2H), 3.41 – 3.33 (m, 2H), 3.23 – 3.18 (m, 1H). ^{13}C NMR (101 MHz, DMSO) δ = 152.8 (q), 149.5 (q), 139.5 (q), 131.9 (+), 131.8 (+), 131.6 (+), 129.9 (+), 128.3 (+), 123.3 (+), 115.7 (+), 84.7 (+), 79.7 (+), 75.2 (+), 70.4 (+), 68.9 (+), 61.1 (-), 28.6 (-). HRMS (ESI) calcd. for ($C_{19}H_{22}N_2O_5SNa^+$) $[M+Na]^+$: m/z = 413.1142; found 413.1143.

(2*R*,3*R*,4*S*,5*R*,6*S*)-2-(hydroxymethyl)-6-((4-((*E*)-phenyldiazenyl)benzyl)thio)tetrahydro-2*H*-pyran-3,4,5-triol (38)

Orange solid (52%). Gradient 0-20 min 10:90 - 98:2, t_R = 10.6 min. m.p. 128 °C. ^{1}H NMR (400 MHz, DMSO-d_6) δ = 7.93 – 7.80 (m, 4H), 7.63 – 7.53 (m, 5H), 4.98 (d, *J* = 5.9 Hz, 1H), 4.79 (d, *J* = 5.5 Hz, 1H), 4.69 (t, *J* = 5.7 Hz, 1H), 4.44 (d, *J* = 4.4 Hz, 1H), 4.09 – 3.98 (m, 2H), 3.87 (d, *J* = 13.0 Hz, 1H), 3.68 (t, *J* = 3.8 Hz, 1H), 3.62 – 3.50 (m, 2H), 3.44 – 3.38 (m, 1H), 3.34 – 3.31 (m, 1H), 3.26 – 3.20 (m, 1H). ^{13}C NMR (101 MHz, DMSO) δ = 152.4 (q), 151.1 (q), 143.2 (q), 131.9 (+), 130.6 (+), 130.9 (+), 123.1 (+), 123.0 (+), 84.0 (+), 79.9 (+), 75.2 (+), 70.5 (+), 69.0 (+), 61.3 (-), 32.5 (-). HRMS (ESI) calcd. for ($C_{19}H_{22}N_2O_5SNa^+$) $[M+Na]^+$: m/z = 413.1142; found 413.1143.

(2*S*,3*R*,4*S*,5*R*,6*R*)-2-((2-((*E*)-(4-(tert-butyl)phenyl)diazenyl)benzyl)thio)-6-(hydroxymethyl)tetrahydro-2*H*-pyran-3,4,5-triol (39)

Light brown solid (16%). Gradient 0-20 min 10:90 - 98:2, t_R = 14.8 min. m.p. 143 °C. ^{1}H NMR (400 MHz, DMSO-d_6) δ = 7.90 – 7.82 (m, 2H), 7.64 – 7.58 (m, 3H), 7.54 (dd, *J* = 7.7, 1.5 Hz, 1H), 7.46 (td, *J* = 7.4, 1.4 Hz, 1H), 7.39 (td, *J* = 7.6, 1.5 Hz, 1H), 4.88 (d, *J* = 5.9 Hz, 1H), 4.75 (d, *J* = 5.6 Hz, 1H), 4.66 (t, *J* = 5.6 Hz, 1H), 4.43 – 4.35 (m, 2H), 4.30 (d, *J* = 12.6 Hz, 1H), 4.14 (d, *J* = 9.5 Hz, 1H), 3.67 (t, *J* = 3.9 Hz, 1H), 3.53 (t, *J* = 5.7 Hz, 2H), 3.40 – 3.34 (m, 2H), 3.22 – 3.16 (m, 1H), 1.33 (s, 9H). ^{13}C NMR (101 MHz, DMSO) δ = 154.5 (q), 150.4 (q), 149.1 (q), 138.8 (q), 131.1 (+), 131.1 (+), 127.8 (+), 126.3 (+), 122.6 (+), 115.2 (+), 84.3 (+), 79.3 (+), 74.7 (+), 70.0 (+), 68.4 (+), 60.6 (-), 34.8 (q), 31.0 (+), 28.2 (-). HRMS (ESI) calcd. for ($C_{23}H_{30}N_2O_5SNa^+$) $[M+Na]^+$: m/z = 469.1768; found 469.1769.

(2*R*,3*R*,4*S*,5*R*,6*S*)-2-(hydroxymethyl)-6-((2-((*E*)-phenyldiazenyl)phenyl)thio)tetrahydro-2*H*-pyran-3,4,5-triol (40)

Orange solid (16%). Gradient 0-10 min 32:68 - 78:22, t_R = 5.8 min. m.p. 166 °C. ^{1}H NMR (400 MHz, DMSO-d_6) δ = 7.90 – 7.86 (m, 2H), 7.72 (dd, *J* = 8.2, 1.2 Hz, 1H), 7.64 – 7.56 (m, 4H), 7.47 (ddd, *J* = 8.3, 7.3, 1.5 Hz, 1H), 7.27 (ddd, *J* = 8.2, 7.2, 1.2 Hz, 1H), 5.26 (d, *J* = 6.0 Hz, 1H), 4.96 (s, 1H), 4.86 (d, *J* = 9.7 Hz, 1H), 4.67 (t, *J* = 5.4 Hz, 1H), 4.55 (d, *J* = 4.5 Hz, 1H), 3.77 (t, *J* = 3.7 Hz, 1H), 3.64 – 3.48 (m, 4H), 3.46 – 3.41 (m, 1H). ^{13}C NMR (101 MHz, DMSO) δ = 152.6 (q), 148.6 (q), 139.7 (q), 132.5 (+), 132.1 (+), 130.0 (+), 127.8 (+), 125.7 (+), 123.2 (+), 116.6 (+), 85.3 (+), 79.6 (+), 75.3 (+), 69.7 (+), 68.9 (+), 61.0 (-). HRMS (ESI) calcd. for ($C_{18}H_{20}N_2O_5SNa^+$) $[M+Na]^+$: m/z = 399.0985; found 399.0986.

(2*R*,3*R*,4*S*,5*R*,6*S*)-2-(hydroxymethyl)-6-((4-((*E*)-phenyldiazenyl)phenyl)thio)tetrahydro-2*H*-pyran-3,4,5-triol (41)

Orange solid (54%). Gradient 0-10 min 23:77 – 67:33, t_R = 8.2 min. m.p. 188 °C. ^{1}H NMR (400 MHz, DMSO-d_6) δ = 7.90 – 7.85 (m, 2H), 7.85 – 7.81 (m, 2H), 7.65 – 7.54 (m, 5H), 5.26 (d, *J* = 6.1 Hz, 1H), 4.94

(d, *J* = 5.7 Hz, 1H), 4.78 (d, *J* = 9.6 Hz, 1H), 4.68 (t, *J* = 5.4 Hz, 1H), 4.55 (d, *J* = 4.4 Hz, 1H), 3.75 (t, *J* = 3.9 Hz, 1H), 3.60 – 3.49 (m, 4H), 3.44 – 3.38 (m, 1H). ^{13}C NMR (101 MHz, DMSO) δ = 152.4 (q), 150.2 (q), 141.3 (q), 131.9 (+), 129.9 (+), 129.1 (+), 123.4 (+), 123.0 (+), 87.1 (+), 79.8 (+), 75.1 (+), 69.6 (+), 68.9 (+), 61.0 (-). HRMS (ESI) calcd. for ($C_{18}H_{21}N_2O_5S^+$) [M+H]$^+$: m/z = 377.1166; found 377.1164.

(2*S*,3*R*,4*S*,5*R*,6*R*)-2-((4-((*E*)-(4-(tert-butyl)phenyl)diazenyl)phenyl)thio)-6-(hydroxymethyl)tetrahydro-2*H*-pyran-3,4,5-triol (42)

Orange solid (39%). Gradient 0-20 min 10:90 -98:2, t_R = 9.7 min. m.p. 146 °C. ^{1}H NMR (400 MHz, DMSO-d_6) δ = 7.85 – 7.77 (m, 4H), 7.64 – 7.58 (m, 4H), 5.26 (d, *J* = 6.0 Hz, 1H), 4.94 (d, *J* = 5.3 Hz, 1H), 4.77 (d, *J* = 9.6 Hz, 1H), 4.68 (t, *J* = 5.5 Hz, 1H), 4.55 (d, *J* = 4.4 Hz, 1H), 3.75 (t, *J* = 3.8 Hz, 1H), 3.58 – 3.48 (m, 4H), 3.44 – 3.39 (m, 1H), 1.33 (s, 9H). ^{13}C NMR (101 MHz, DMSO) δ = 154.9 (q), 150.4 (q), 150.3 (q), 140.8 (q), 129.2 (+), 126.7 (+), 123.3 (+), 122.8 (+), 87.2 (+), 79.8 (+), 75.1 (+), 69.7 (+), 68.8 (+), 61.0 (-), 35.3 (+), 31.4 (+). HRMS (ESI) calcd. for ($C_{22}H_{28}N_2O_5SNa^+$) [M+Na]$^+$: m/z = 455.1611; found 455.1610.

(*E*)-2,2'-(diazene-1,2-diylbis(4,1-phenylene))bis(ethan-1-ol) (45)

The symmetric phenethyl-alcohol azobenzene **45** was synthesized in a twostep procedure starting from 2-(4-aminophenyl)ethan-1-ol (**43**). In order to perform a Mills reaction the amino-group of **43** was transformed into its nitroso derivative following an adapted literature procedure.[10] The PhSeSePh catalyst (57 mg, 5.0 mol-%), the aniline **43** (0.50 g, 3.6 mmol, 1.0 eq), and 30% aqueous H_2O_2 (0.24 mL, 7.9 mmol, 2.2 eq) were mixed $CHCl_3$/MeCN (1:1, 5.0 mL) and stirred at room temperature for one hour. The solvent was evaporated and the generated nitroso **44** was used without further purification. For the following Mills reaction the nitroso-derivative **44** was dissolved in acetic acid (15 mL) and the aniline **43** (0.50 g, 3.6 mmol, 1.0 eq) was added and the mixture stirred at room temperature for 16 hours. Purification by flash column chromatography (CH_2Cl_2) afforded the desired product **45** as orange solid in moderate yield (389 mg, 1.4 mmol, 40%). ^{1}H NMR (400 MHz, DMSO-d_6) δ = 7.80 (d, *J* = 8.3 Hz, 4H), 7.43 (d, *J* = 8.4 Hz, 4H), 4.70 (t, *J* = 5.2 Hz, 2H), 3.71 – 3.60 (m, 4H), 2.82 (t, *J* = 6.9 Hz, 4H). ^{13}C NMR (101 MHz, DMSO) δ = 150.4 (q), 143.6 (q), 129.9 (+), 122.3 (+), 61.8 (-), 38.8 (-). HRMS (ESI) calcd. for ($C_{16}H_{18}N_2O_2Na^+$) [M+Na]$^+$: m/z = 293.1260; found 293.1261.

(*E*)-1,2-bis(4-(2-bromoethyl)phenyl)diazene (46)

Compound **46** was synthesized according to a literature adapted procedure.[11] A solution of triphenyl phosphine (1.1 g, 4.2 mmol, 3.0 eq) was dissolved in anhydrous CH_2Cl_2 (10 mL) and added to a suspension of the symmetric phenethyl-alcohol azobenzene **45** (0.39 g, 1.4 mmol, 1.0 eq) and tetra bromomethane (1.1 g, 3.4 mmol, 2.4 eq) in anhydrous CH_2Cl_2 (20 mL) under an inert gas atmosphere. The reaction mixture was stirred at room temperature for two hours until TLC indicated full conversion of the starting material. The solution was diluted with CH_2Cl_2, filtered, and concentrated under reduced pressure. Purification by flash column chromatography (CH_2Cl_2) and evaporation of the solvent afforded the desired product **46** as red solid in high yield (0.46 g, 1.1 mmol, 82%). ^{1}H NMR (300 MHz, DMSO-d_6) δ = 7.84 (d, *J* = 8.3 Hz, 4H), 7.50 (d, *J* = 8.4 Hz, 4H), 3.80 (t, *J* = 7.1 Hz, 4H), 3.24 (t, *J* = 7.1 Hz, 4H). ^{13}C NMR (75 MHz, DMSO) δ = 150.8 (q), 142.7 (q), 129.9 (+), 122.5 (+), 38.0 (-), 34.2 (-). HRMS (ESI) calcd. for ($C_{16}H_{16}N_2Br_2Na^+$) [M+Na]$^+$: m/z = 418.9553; found 418.9554.

(2*R*,2'*R*,3*R*,3'*R*,4*S*,4'*S*,5*R*,5'*R*,6*S*,6'*S*)-6,6'-(((((*E*)-diazene-1,2-diyl)bis(4,1-phenylene))bis(ethane-2,1-diyl))bis(sulfanediyl))bis(2-(hydroxymethyl)tetrahydro-2*H*-pyran-3,4,5-triol) (49)

The compound was synthesized in a two step procedure starting from **46** following a literature adapted procedure. Under a nitrogen atmosphere thiourea (0.36 g, 4.4 mmol, 4.0 eq) was added to a solution of symmetric bromoethylazobenezene **46** (0.46 g, 1.1 mmol, 1.0 eq) in ethanol (20 mL) and heated to

reflux for 16 hours. 10% aqueous NaOH (20 mL) was added and the solution heated to reflux for additional two hours.[11] The solvent was removed under reduced pressure and the residue extracted with CH_2Cl_2 and water. The organic phase was dried ($MgSO_4$), filtered, and concentrated under reduced pressure. The orange product (0.24 g, 0.78 mmol, 71%) was directly used in the next step without further purification to avoid disulfide formation or degradation. (*E*)-2-2'-(diazene-1,2-diylbis(4,1-phenylene))bis(ethane-1-thiol) (47) (236 mg, 0.78 mmol, 1.0 eq) was added to a solution of 1,2,3,4,6-penta-*O*-acetyl-D-galactose (**7**) (0.61 g, 1.6 mmol, 2.0 eq) in CH_2Cl_2 (7.0 mL). The reaction mixture was stirred for 15 min at room temperature, cooled to 0 °C and boron trifluoride diethyl etherate (2.0 mL, 5.5 mmol, 7.0 eq) was added dropwise. The mixture was stirred for 15 minutes, warmed to room temperature, and stirred for additional 24 hours. The reaction mixture was diluted with CH_2Cl_2, and poured into ice water under stirring. The organic phase was separated, washed with saturated $NaHCO_3$, water, dried (Na_2SO_4), filtered, and concentrated.[9] Purification by flash column chromatography (CH_2Cl_2 + 10% MeOH) and evaporation of the solvent afforded the pentaacetylated galactopyranose azobenzene derivative **48** (0.36 g, 0.37 mmol, 47%) as orange solid. Deacetylation was achieved by dissolving the compound in MeOH (10 mL) and addition of potassium carbonate (51 mg, 0.37 mmol, 1.0 eq). The reaction mixture was stirred at room temperature for 30 minutes, filtered, and concentrated under reduced pressure. Purification by preparative HPLC (gradient 0-9 min 10:90 – 60:40, t_R = 8.06 min) afforded the desired product as orange solid in quantitative yield (0.23 g, 0.37 mmol). m.p. 202 °C. ^{1}H NMR (400 MHz, DMSO-d_6) δ = 7.81 (d, *J* = 8.3 Hz, 4H), 7.47 (d, *J* = 8.4 Hz, 4H), 4.96 (d, *J* = 5.7 Hz, 2H), 4.79 (d, *J* = 5.4 Hz, 2H), 4.60 (t, *J* = 5.6 Hz, 2H), 4.41 (d, *J* = 4.4 Hz, 2H), 4.28 (d, *J* = 9.4 Hz, 2H), 3.69 (t, *J* = 3.9 Hz, 2H), 3.51 (t, *J* = 5.4 Hz, 4H), 3.42 – 3.35 (m, 4H), 3.32 – 3.27 (m, 2H), 3.02 – 2.92 (m, 6H), 2.91 – 2.81 (m, 2H). ^{13}C NMR (101 MHz, DMSO) δ = 151.0 (q), 145.1 (q), 130.1 (+), 122.9 (+), 86.1 (+), 79.7 (+), 75.2 (+), 70.2 (+), 68.9 (+), 61.1 (-), 36.3 (-), 30.7 (-). HRMS (ESI) calcd. for ($C_{28}H_{39}N_2O_{10}^+$) $[M+H]^+$: m/z = 627.2041; found 627.2040.

Enzymatic inhibition studies

A 2 µM β-galactosidase stock solution was diluted to 720 pM in sterile filtered assay buffer (137 mM NaCl, 10 mM Na_2HPO_4, 2 mM KH_2PO_4, 2.7 mM KCl, pH 7.5) containing 0.05 mg mL^{-1} bovine serum albumin, 0.005% Tween 20 and 1 mM $MgCl_2$. Prior to each measurement, 10 µl of β-galactosidase was added to 190 µl of substrate or substrate / inhibitor mix resulting in a final enzyme concentration of 36 pM. Inhibitors were dissolved in DMSO to a concentration of 20 mM, diluted in assay buffer and mixed either directly 1:1 with the substrate (*trans*-isomer in its thermal equilibrium) or irradiated at 365 nm for 1 minute in a fused silica microplate and then mixed with the substrate (*cis*-isomer at its photostationary state). Fluorescence measurements (λ_{exc}: 565 nm; λ_{em}: 590 nm) were performed in a Synergy neo 2 multi-mode microplate reader (BioTek) at 25 °C. The formation of the fluorescent product resorufin was observed in intervals of 30 s over a period of 5 minutes. The inhibitory activity of all compounds was pre-tested at a concentration of typically 100 µM (Table S4). Three of these compounds showed a high inhibitory activity and were investigated in detail. The initial increase of the fluorescence was normalized to the uninhibited reaction and the inhibitor concentrations [I] were varied at 3 different substrate concentrations ([S] = 50, 100 and 150 µM). K_i values were determined by non-linear regression using the Michaelis Menten model for competitive inhibition (Eq. 1). The velocity at substrate saturation (V_{max}) was set to 1000 s^{-1} [12] and the Michaelis constant K_M was determined as a curve fit parameter.

$$v = \frac{V_{max} \cdot [S]}{K_M \cdot \left(1 + \frac{[I]}{K_i}\right) + [S]} \qquad \text{Eq. 1}$$

Molecular docking

The ligands were docked to an ensemble of β-galactosidases using VINA[13] as implemented in YASARA[14]. The ensemble consisted of the following 3D structures indicated by their PDB IDs: 1dp0, 1f4a, 1f4h, 1hn1, 1jyn, 1jyv, 1jyw, 1jyx, 1jz2, 1jz3, 1jz4, 1jz5, 1jz6, 1jz7, 1jz8, 1px3, 1px4, 3czj, 3dym, 3dyo, 3dyp, 3e1f, 3i3b, 3i3d, 3i3e, 3iap, 3iaq, 3j7h, 3muy, 3muz, 3mv0, 3mv1, 3sep, 3t08, 3t09, 3t0a, 3t0b, 3t0d, 3t2o, 3t2p, 3t2q, 3vd3, 3vd4, 3vd5, 3vd7, 3vd9, 3vda, 3vdb, 3vdc, 4ckd, 4duv, 4duw, 4dux, 4ttg, 5a1a. Residues with a distance of ≤ 10 Å to the ligand-binding site were made flexible; all other ones were kept rigid. For a comprehensive sampling of the search space, every ligand was docked 32 times to each receptor, resulting in 1760 dockings per ligand. The results were ranked according to their estimated dissociation constant.

UV-Vis Absorption Spectroscopic Photochromic Characterization.

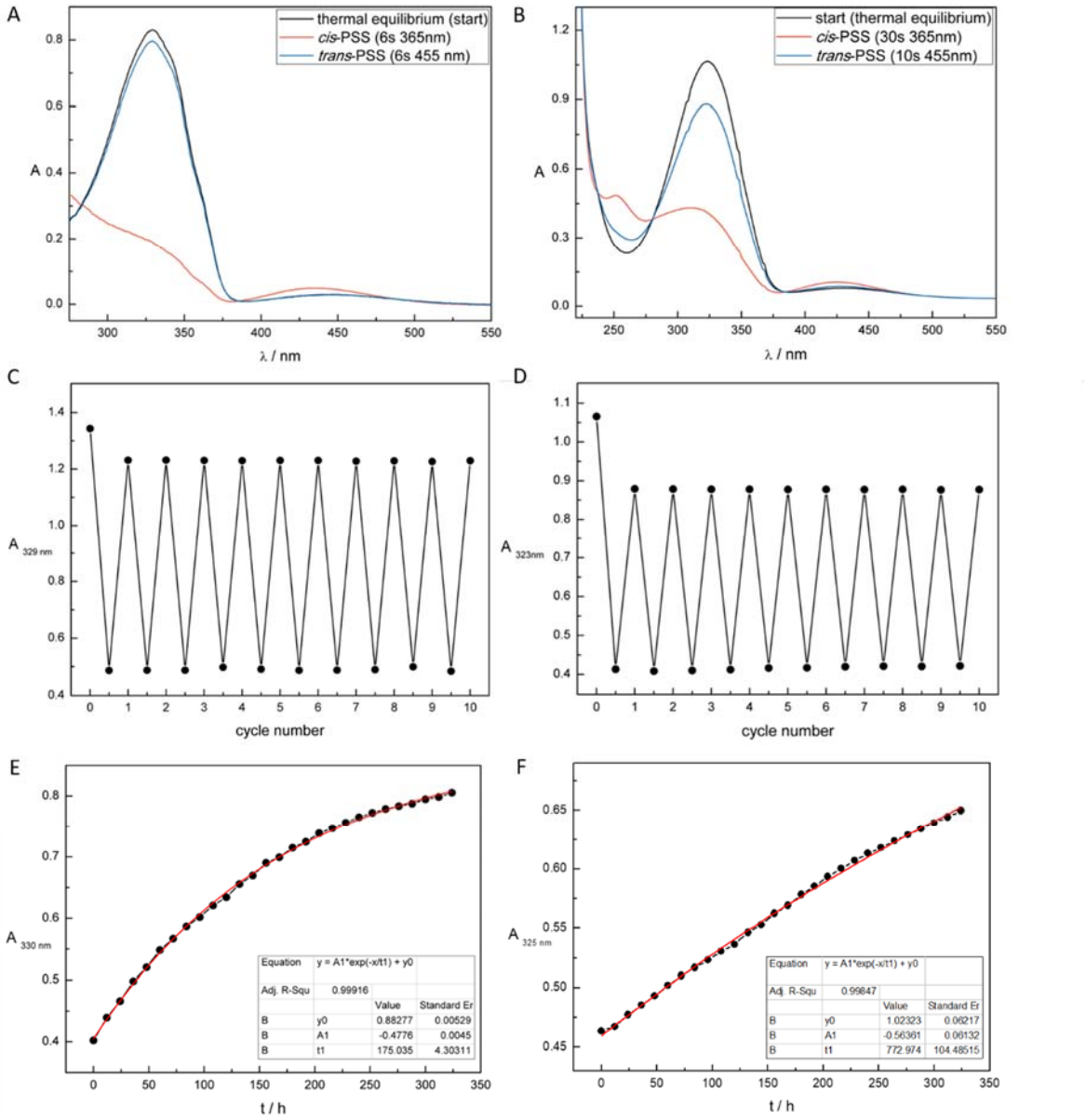

Figure S1. **Changes in absorption spectra of 4 upon continuous irradiation until the PSS is reached.** (A) 50 µM in DMSO. λ (*cis*-PSS) = 365 nm, λ (*trans*-PSS) = 455 nm. (B) 50 µM in phosphate buffer + 0.1% DMSO. λ (*cis*-PSS) = 365 nm, λ (*trans*-PSS) = 455 nm. **Cycle performance of 4.** (C) 50 µM in DMSO. Changes in absorption at 329 nm (λ_{max} of the *trans*-isomer) were measured during alternate irradiation with light of λ = 365 nm and λ = 455 nm until the PSS is reached. (D) 50 µM in phosphate buffer + 0.1% DMSO. Changes in absorption at 323 nm (λ_{max} of the *trans*-isomer) were measured during alternate irradiation with light of λ = 365 nm and λ = 455 nm until the PSS is reached. **Thermal stability of the *cis*-isomer of 4 measured at 25 °C**. Black dots represent the absorption at the indicated wavelength dependent on the time of relaxation [h]. Red curve represents an exponential nonlinear curve fit. (E) 50 µM in DMSO. Changes in absorption maxima measured at 330 nm (λ_{max} of the *trans*-isomer) after irradiation with λ = 365 nm until the PSS is reached. $t_{0.5}$ = 121 h. (F) 50 µM solution in phosphate buffer + 0.1% DMSO. Changes in absorption maxima measured at 323 nm (λ_{max} of the *trans*-isomer) after irradiation with λ = 365 nm until the PSS is reached. $t_{0.5}$ = 536 h.

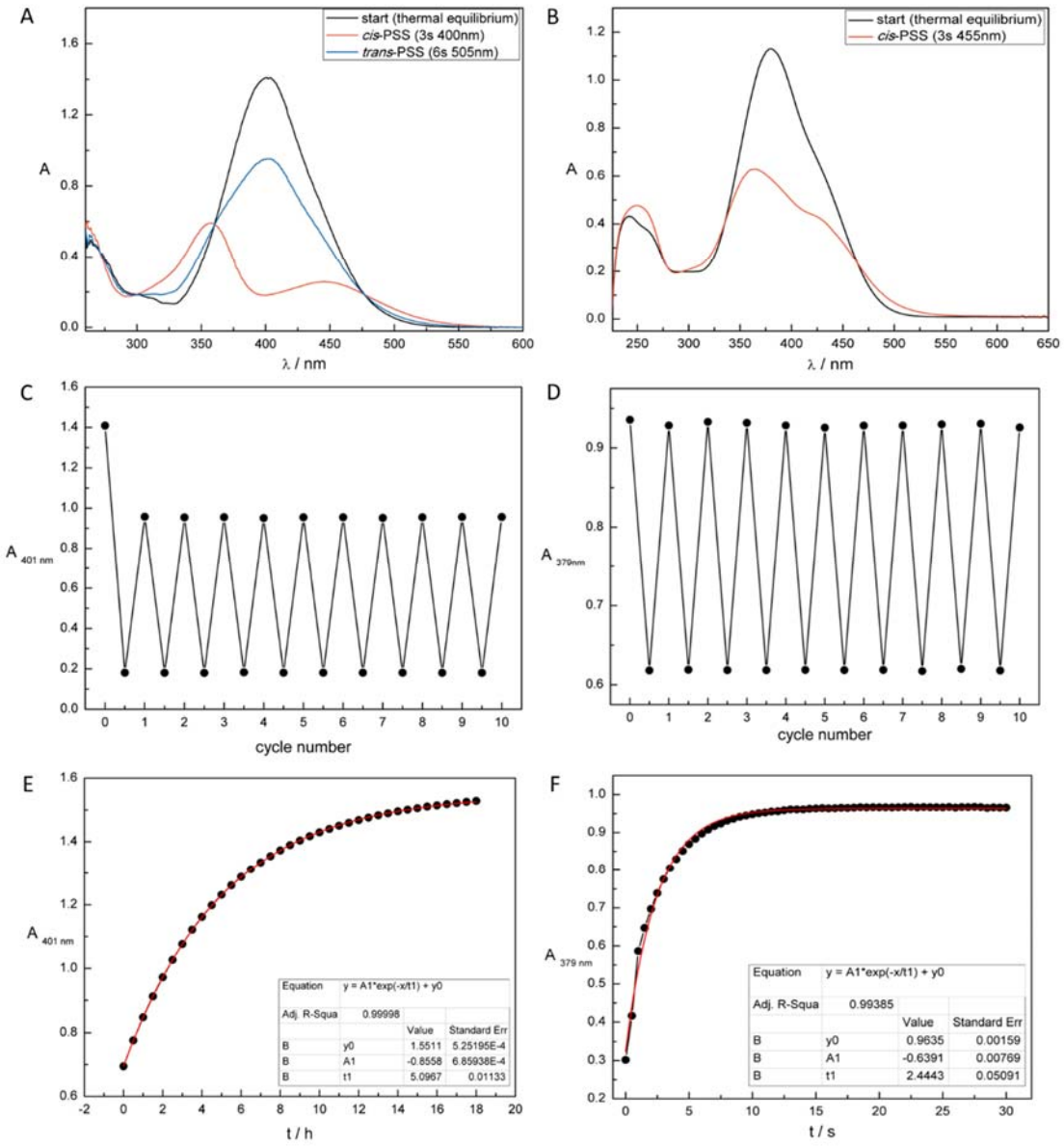

Figure S2. **Changes in absorption spectra of 6 upon continuous irradiation until the PSS is reached.** (A) 50 µM in DMSO. λ (*cis*-PSS) = 400 nm, λ (*trans*-PSS) = 505 nm. (B) 50 µM in phosphate buffer + 0.1% DMSO. λ (*cis*-PSS) = 455 nm. **Cycle performance of 6.** (C) 50 µM in DMSO. Changes in absorption at 401 nm (λ_{max} of the *trans*-isomer) were measured during alternate irradiation with light of λ = 400 nm and λ = 505 nm until the PSS is reached. (D) 25 µM in phosphate buffer + 0.1% DMSO. Changes in absorption at 379 nm (λ_{max} of the *trans*-isomer) were measured during irradiation with light of λ = 455 nm and thermal back relaxation until the PSS is reached. **Thermal stability of the *cis*-isomer of 6 measured at 25 °C**. Black dots represent the absorption at the indicated wavelength dependent on the time of relaxation [h]. Red curve represents an exponential nonlinear curve fit. (E) 50 µM in DMSO. Changes in absorption maxima measured at 401 nm (λ_{max} of the *trans*-isomer) after irradiation with λ = 400 nm until the PSS is reached. $t_{0.5}$ = 3.5 h. (F) 50 µM solution in phosphate buffer + 0.1% DMSO. Changes in absorption maxima measured at 379 nm (λ_{max} of the *trans*-isomer) after irradiation with λ = 455 nm until the PSS is reached. $t_{0.5}$ = 1.69 s.

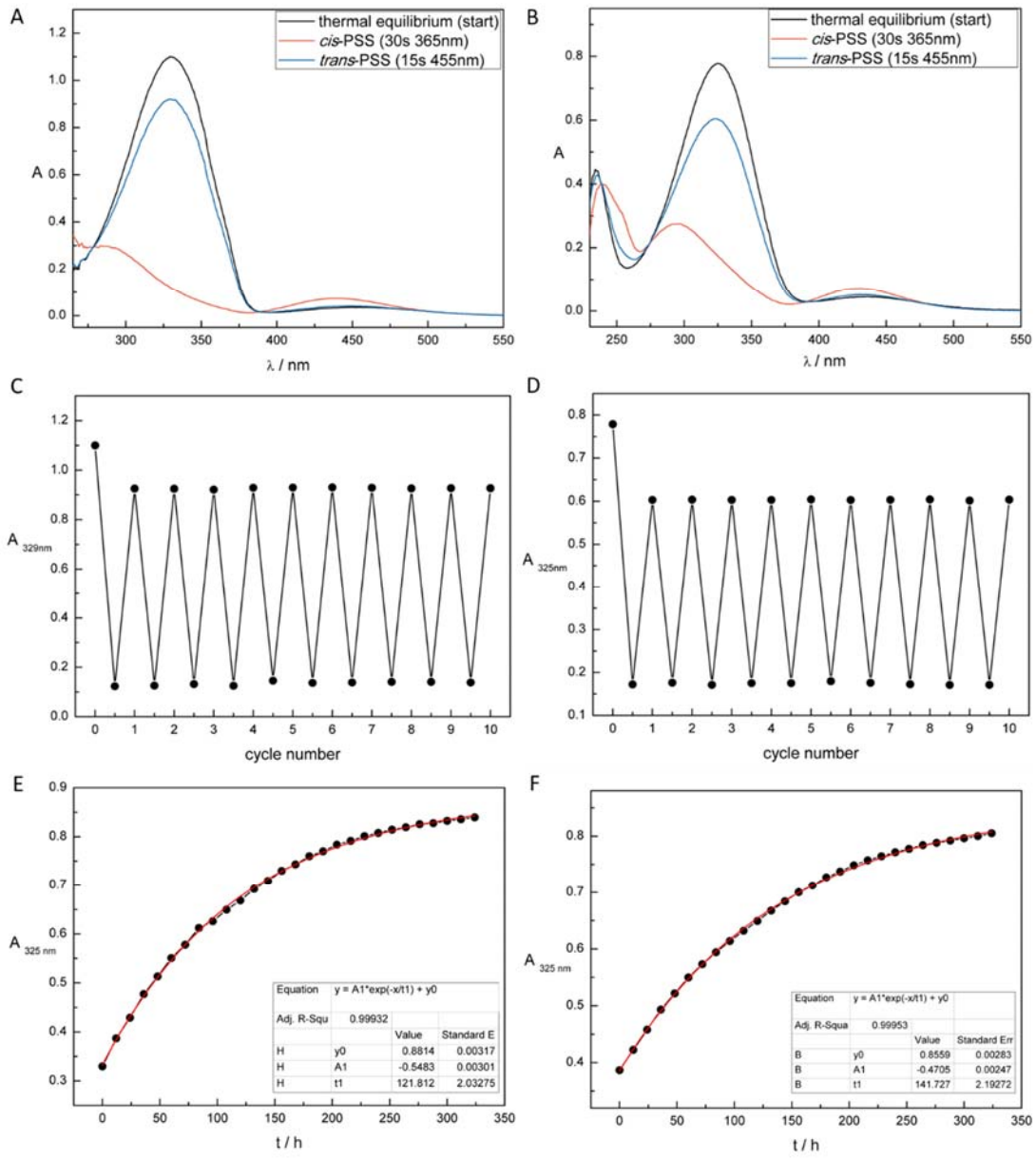

Figure S3. **Changes in absorption spectra of 34 upon continuous irradiation until the PSS is reached.** (A) 50 µM in DMSO. λ (*cis*-PSS) = 365 nm, λ (*trans*-PSS) = 455 nm. (B) 50 µM in phosphate buffer + 0.1% DMSO. λ (*cis*-PSS) = 365 nm, λ (*trans*-PSS) = 455 nm. **Cycle performance of 34.** (C) 50 µM in DMSO. Changes in absorption at 329 nm (λ_{max} of the *trans*-isomer) were measured during alternate irradiation with light of λ = 365 nm and λ = 455 nm until the PSS is reached. (D) 50 µM in phosphate buffer + 0.1% DMSO. Changes in absorption at 325 nm (λ_{max} of the *trans*-isomer) were measured during alternate irradiation with light of λ = 365 nm and λ = 455 nm until the PSS is reached. **Thermal stability of the *cis*-isomer of 34 measured at 25 °C**. Black dots represent the absorption at the indicated wavelength dependent on the time of relaxation [h]. Red curve represents an exponential nonlinear curve fit. (E) 50 µM in DMSO. Changes in absorption maxima measured at 325 nm after irradiation with λ = 365 nm until the PSS is reached. $t_{0.5}$ = 84.4 h. (F) 50 µM solution in phosphate buffer + 0.1% DMSO. Changes in absorption maxima measured at 325 nm (λ_{max} of the *trans*-isomer) after irradiation with λ = 365 nm until the PSS is reached. $t_{0.5}$ = 98.2 h.

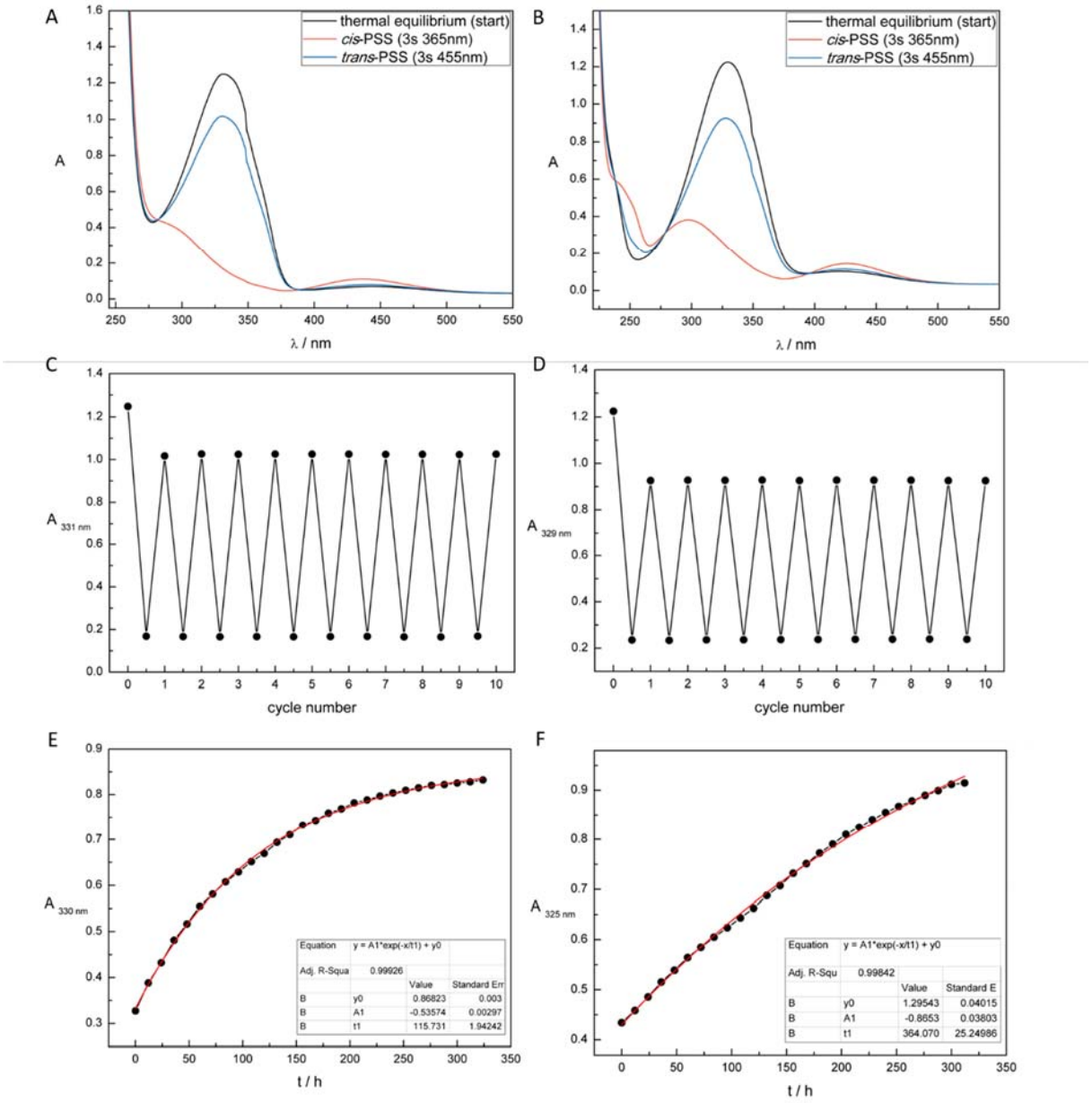

Figure S4. **Changes in absorption spectra of 35 upon continuous irradiation until the PSS is reached.** (A) 50 µM in DMSO. λ (*cis*-PSS) = 365 nm, λ (*trans*-PSS) = 455 nm. (B) 50 µM in phosphate buffer + 0.1% DMSO. λ (*cis*-PSS) = 365 nm, λ (*trans*-PSS) = 455 nm. **Cycle performance of 35.** (C) 50 µM in DMSO. Changes in absorption at 331 nm (λ_{max} of the *trans*-isomer) were measured during alternate irradiation with light of λ = 365 nm and λ = 455 nm until the PSS is reached. (D) 50 µM in phosphate buffer + 0.1% DMSO. Changes in absorption at 329 nm (λ_{max} of the *trans*-isomer) were measured during alternate irradiation with light of λ = 365 nm and λ = 455 nm until the PSS is reached. **Thermal stability of the *cis*-isomer of 35 measured at 25 °C**. Black dots represent the absorption at the indicated wavelength dependent on the time of relaxation [h]. Red curve represents an exponential nonlinear curve fit. (E) 50 µM in DMSO. Changes in absorption maxima measured at 330 nm after irradiation with λ = 365 nm until the PSS is reached. $t_{0.5}$ = 80.2 h. (F) 50 µM solution in phosphate buffer + 0.1% DMSO. Changes in absorption maxima measured at 325 nm after irradiation with λ = 365 nm until the PSS is reached. $t_{0.5}$ = 252 h.

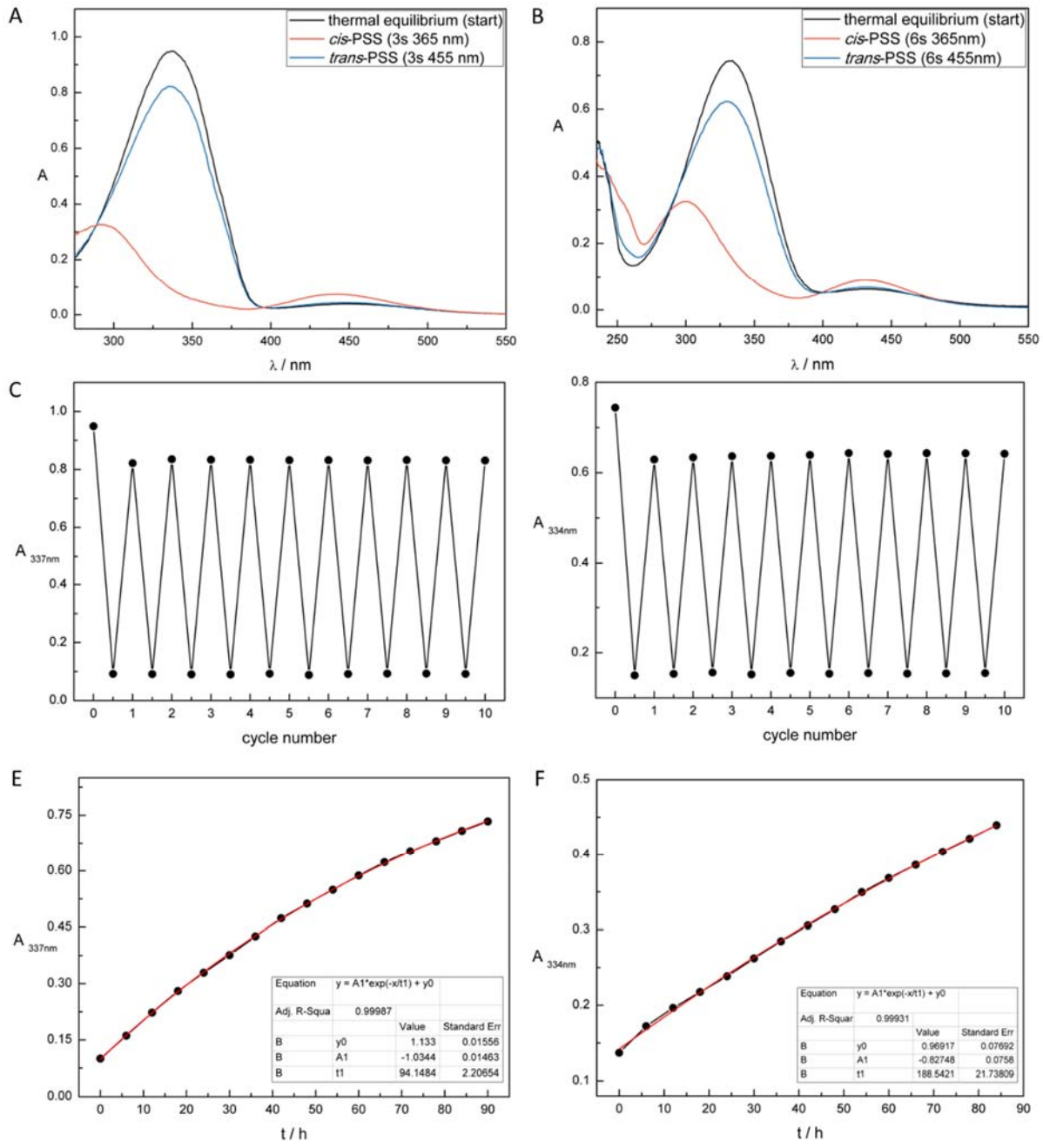

Figure S5. **Changes in absorption spectra of 36 upon continuous irradiation until the PSS is reached.** (A) 50 µM in DMSO. λ (*cis*-PSS) = 365 nm, λ (*trans*-PSS) = 455 nm. (B) 50 µM in phosphate buffer + 1% DMSO. λ (*cis*-PSS) = 365 nm, λ (*trans*-PSS) = 455 nm. **Cycle performance of 36.** (C) 50 µM in DMSO. Changes in absorption at 337 nm (λ_{max} of the *trans*-isomer) were measured during alternate irradiation with light of λ = 365 nm and λ = 455 nm until the PSS is reached. (D) 50 µM in phosphate buffer + 1% DMSO. Changes in absorption at 334 nm (λ_{max} of the *trans*-isomer) were measured during alternate irradiation with light of λ = 365 nm and λ = 455 nm until the PSS is reached. **Thermal stability of the *cis*-isomer of 36 measured at 25 °C**. Black dots represent the absorption at the indicated wavelength dependent on the time of relaxation [h]. Red curve represents an exponential nonlinear curve fit. (E) 50 µM in DMSO. Changes in absorption maxima measured at 337 nm (λ_{max} of the *trans*-isomer) after irradiation with λ = 365 nm until the PSS is reached. $t_{0.5}$ = 65.2 h. (F) 50 µM solution in phosphate buffer + 1% DMSO. Changes in absorption maxima measured at 334 nm after irradiation with λ = 365 nm until the PSS is reached. $t_{0.5}$ = 131 h.

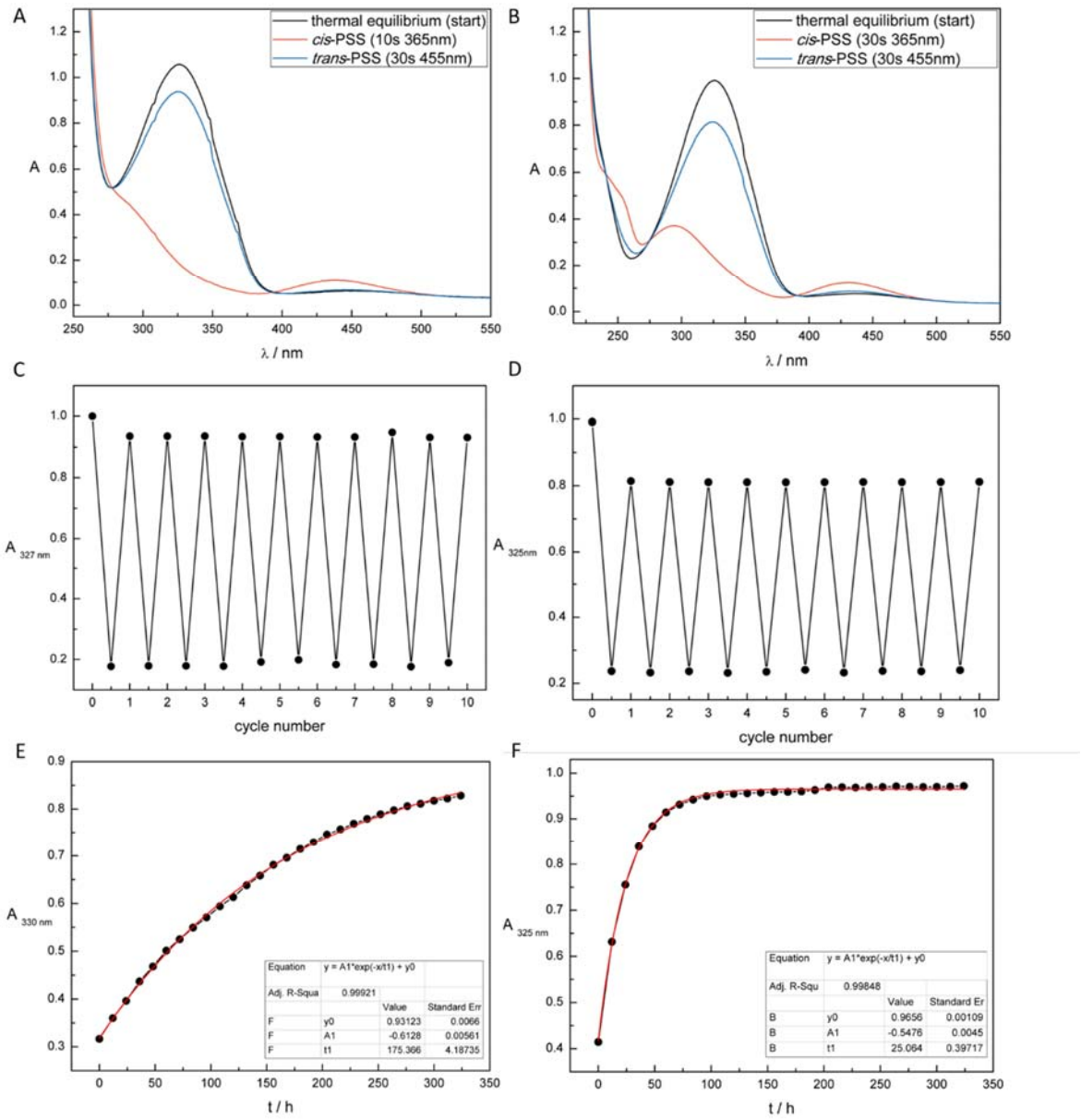

Figure S6. **Changes in absorption spectra of 37 upon continuous irradiation until the PSS is reached.** (A) 50 µM in DMSO. λ (*cis*-PSS) = 365 nm, λ (*trans*-PSS) = 455 nm. (B) 50 µM in phosphate buffer + 0.1% DMSO. λ (*cis*-PSS) = 365 nm, λ (*trans*-PSS) = 455 nm. **Cycle performance of 37.** (C) 50 µM in DMSO. Changes in absorption at 327 nm (λ_{max} of the *trans*-isomer) were measured during alternate irradiation with light of λ = 365 nm and λ = 455 nm until the PSS is reached. (D) 50 µM in phosphate buffer + 0.1% DMSO. Changes in absorption at 325 nm (λ_{max} of the *trans*-isomer) were measured during alternate irradiation with light of λ = 365 nm and λ = 455 nm until the PSS is reached. **Thermal stability of the *cis*-isomer of 37 measured at 25 °C**. Black dots represent the absorption at the indicated wavelength dependent on the time of relaxation [h]. Red curve represents an exponential nonlinear curve fit. (E) 50 µM in DMSO. Changes in absorption maxima measured at 340 nm after irradiation with λ = 365 nm until the PSS is reached. $t_{0.5}$ = 122 h. (F) 50 µM solution in phosphate buffer + 0.1% DMSO. Changes in absorption maxima measured at 325 nm (λ_{max} of the *trans*-isomer) after irradiation with λ = 365 nm until the PSS is reached. $t_{0.5}$ = 17.4 h.

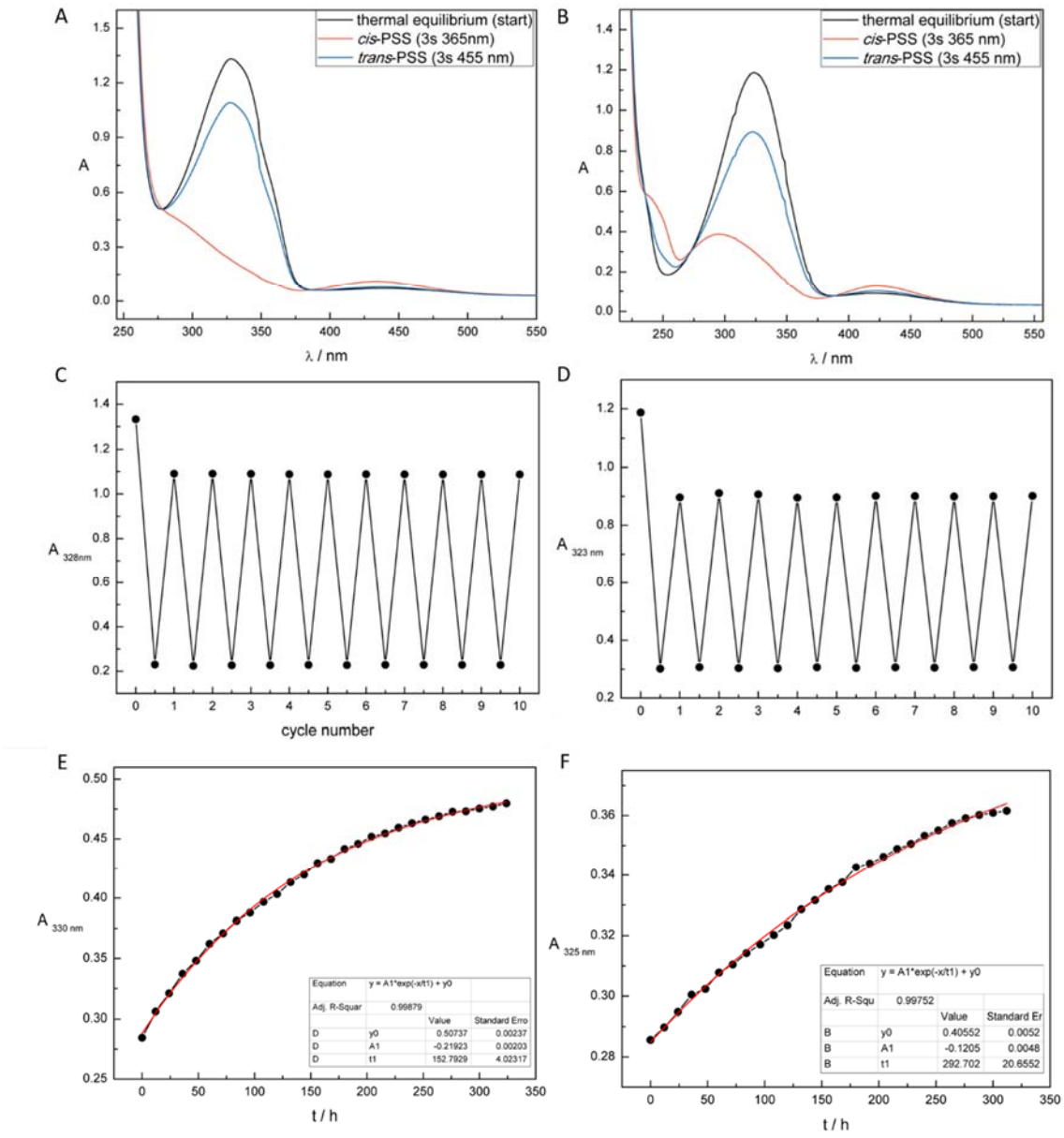

Figure S7. **Changes in absorption spectra of 38 upon continuous irradiation until the PSS is reached.** (A) 50 µM in DMSO. λ (*cis*-PSS) = 365 nm, λ (*trans*-PSS) = 455 nm. (B) 50 µM in phosphate buffer + 0.1% DMSO. λ (*cis*-PSS) = 365 nm, λ (*trans*-PSS) = 455 nm. **Cycle performance of 38.** (C) 50 µM in DMSO. Changes in absorption at 328 nm (λ_{max} of the *trans*-isomer) were measured during alternate irradiation with light of λ = 365 nm and λ = 455 nm until the PSS is reached. (D) 50 µM in phosphate buffer + 0.1% DMSO. Changes in absorption at 323 nm (λ_{max} of the *trans*-isomer) were measured during alternate irradiation with light of λ = 365 nm and λ = 455 nm until the PSS is reached. **Thermal stability of the *cis*-isomer of 38 measured at 25 °C**. Black dots represent the absorption at the indicated wavelength dependent on the time of relaxation [h]. Red curve represents an exponential nonlinear curve fit. (E) 50 µM in DMSO. Changes in absorption maxima measured at 330 nm after irradiation with λ = 365 nm until the PSS is reached. $t_{0.5}$ = 106 h. (F) 50 µM solution in phosphate buffer + 0.1% DMSO. Changes in absorption maxima measured at 325 nm after irradiation with λ = 365 nm until the PSS is reached. $t_{0.5}$ = 203 h.

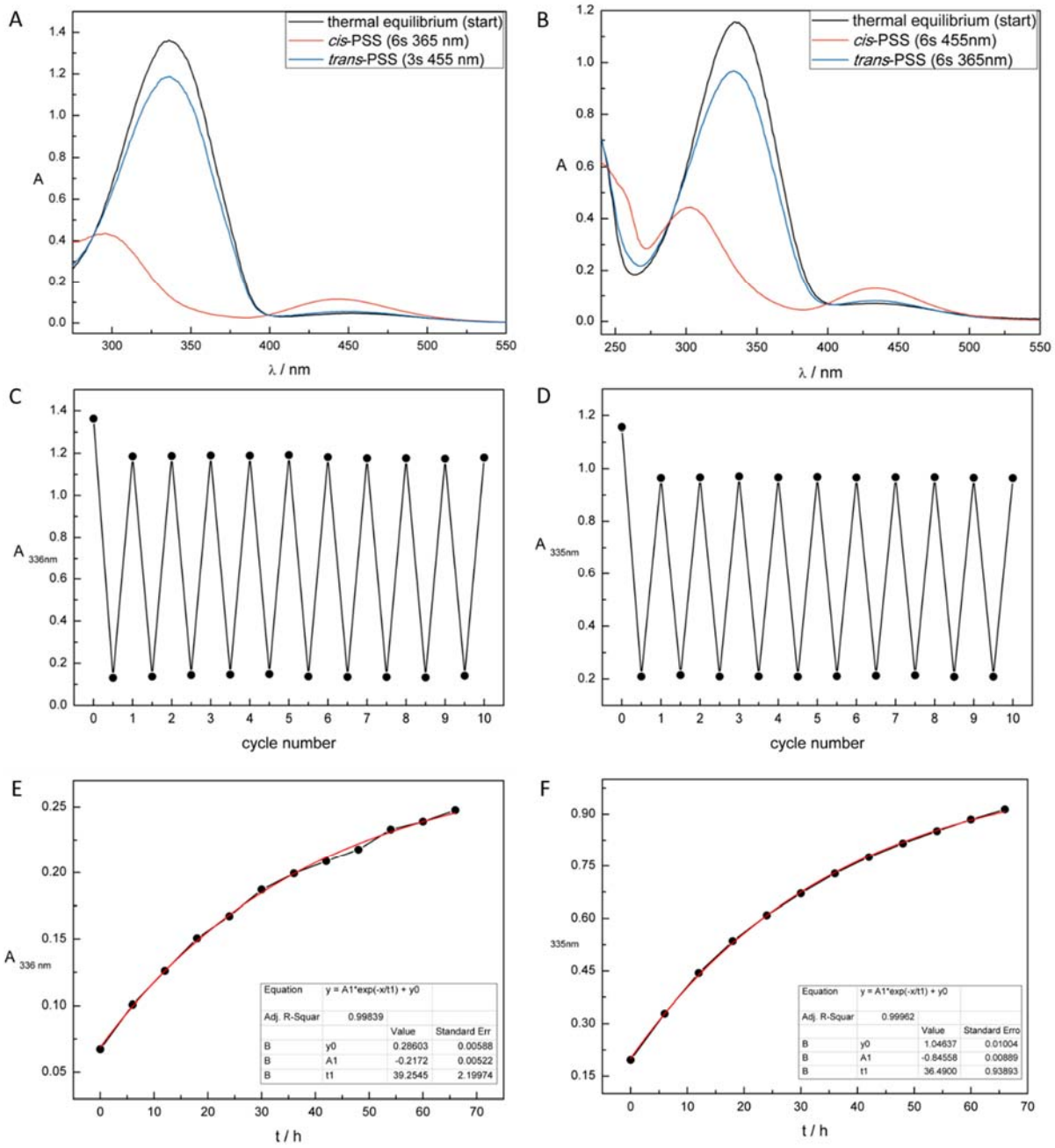

Figure S8. **Changes in absorption spectra of 39 upon continuous irradiation until the PSS is reached.** (A) 50 µM in DMSO. λ (*cis*-PSS) = 336 nm, λ (*trans*-PSS) = 446 nm. (B) 50 µM in phosphate buffer + 1% DMSO. λ (*cis*-PSS) = 335 nm, λ (*trans*-PSS) = 434 nm. **Cycle performance of 39.** (C) 50 µM in DMSO. Changes in absorption at 336 nm (λ_{max} of the *trans*-isomer) were measured during alternate irradiation with light of λ = 365 nm and λ = 455 nm until the PSS is reached. (D) 50 µM in phosphate buffer + 1% DMSO. Changes in absorption at 335 nm (λ_{max} of the *trans*-isomer) were measured during alternate irradiation with light of λ = 365 nm and λ = 455 nm until the PSS is reached. **Thermal stability of the *cis*-isomer of 39 measured at 25 °C**. Black dots represent the absorption at the indicated wavelength dependent on the time of relaxation [h]. Red curve represents an exponential nonlinear curve fit. (E) 25 µM in DMSO. Changes in absorption maxima measured at 336 nm (λ_{max} of the *trans*-isomer) after irradiation with λ = 365 nm until the PSS is reached. $t_{0.5}$ = 27.2 h. (F) 50 µM solution in phosphate buffer + 1% DMSO. Changes in absorption maxima measured at 350 nm after irradiation with λ = 365 nm until the PSS is reached. $t_{0.5}$ = 25.3 h.

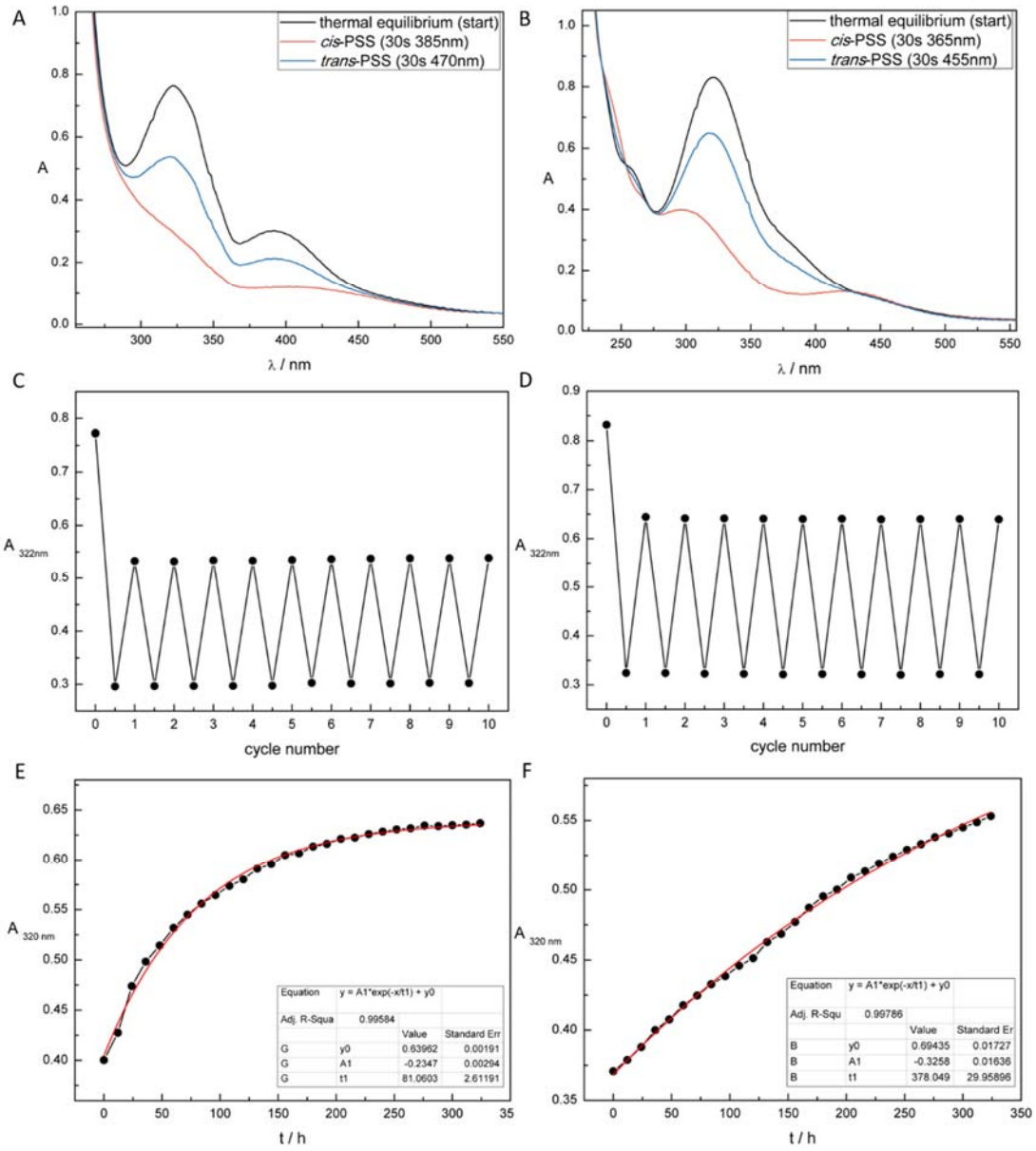

Figure S9. **Changes in absorption spectra of 40 upon continuous irradiation until the PSS is reached.** (A) 50 µM in DMSO. λ (*cis*-PSS) = 385 nm, λ (*trans*-PSS) = 470 nm. (B) 50 µM in phosphate buffer + 0.1% DMSO. λ (*cis*-PSS) = 365 nm, λ (*trans*-PSS) = 455 nm. **Cycle performance of 40.** (C) 50 µM in DMSO. Changes in absorption at 322 nm (λ_{max} of the *trans*-isomer) were measured during alternate irradiation with light of λ = 385 nm and λ = 470 nm until the PSS is reached. (D) 50 µM in phosphate buffer + 0.1% DMSO. Changes in absorption at 322 nm (λ_{max} of the *trans*-isomer) were measured during alternate irradiation with light of λ = 365 nm and λ = 455 nm until the PSS is reached. **Thermal stability of the *cis*-isomer of 40 measured at 25 °C**. Black dots represent the absorption at the indicated wavelength dependent on the time of relaxation [h]. Red curve represents an exponential nonlinear curve fit. (E) 50 µM in DMSO. Changes in absorption maxima measured at 320 nm after irradiation with λ = 385 nm until the PSS is reached. $t_{0.5}$ = 56.2 h. (F) 50 µM solution in phosphate buffer + 0.1% DMSO. Changes in absorption maxima measured at 320 nm after irradiation with λ = 365 nm until the PSS is reached. $t_{0.5}$ = 262 h.

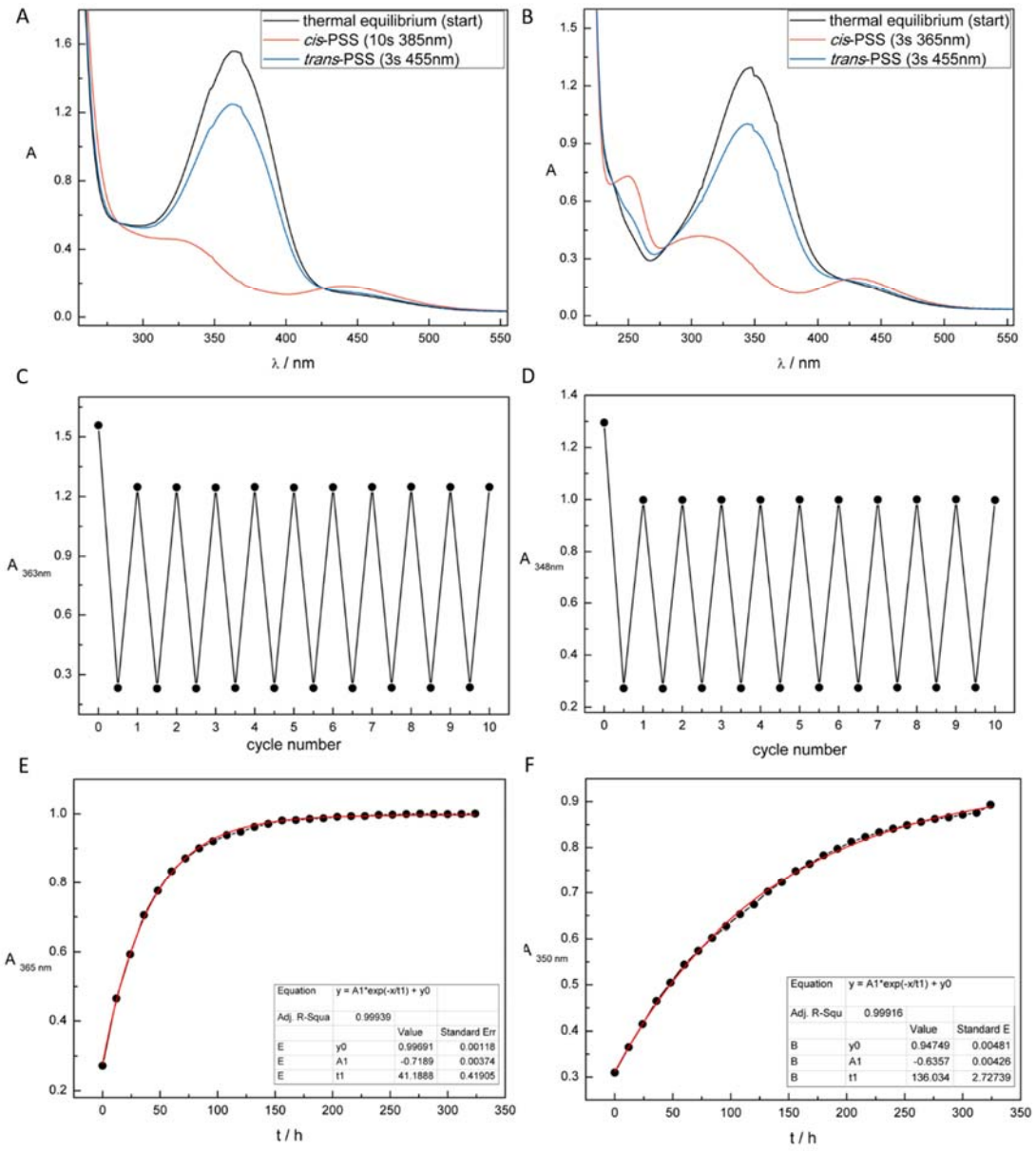

Figure S10. **Changes in absorption spectra of 41 upon continuous irradiation until the PSS is reached.** (A) 50 µM in DMSO. λ (*cis*-PSS) = 385 nm, λ (*trans*-PSS) = 455 nm. (B) 50 µM in phosphate buffer + 0.1% DMSO. λ (*cis*-PSS) = 365 nm, λ (*trans*-PSS) = 455 nm. **Cycle performance of 41.** (C) 50 µM in DMSO. Changes in absorption at 363 nm (λ_{max} of the *trans*-isomer) were measured during alternate irradiation with light of λ = 365 nm and λ = 455 nm until the PSS is reached. (D) 50 µM in phosphate buffer + 0.1% DMSO. Changes in absorption at 348 nm (λ_{max} of the *trans*-isomer) were measured during alternate irradiation with light of λ = 365 nm and λ = 455 nm until the PSS is reached. **Thermal stability of the *cis*-isomer of 41 measured at 25 °C**. Black dots represent the absorption at the indicated wavelength dependent on the time of relaxation [h]. Red curve represents an exponential nonlinear curve fit. (E) 50 µM in DMSO. Changes in absorption maxima measured at 365 nm after irradiation with λ = 385 nm until the PSS is reached. $t_{0.5}$ = 28.5 h. (F) 50 µM solution in phosphate buffer + 0.1% DMSO. Changes in absorption maxima measured at 350 nm after irradiation with λ = 365 nm until the PSS is reached. $t_{0.5}$ = 94.3 h.

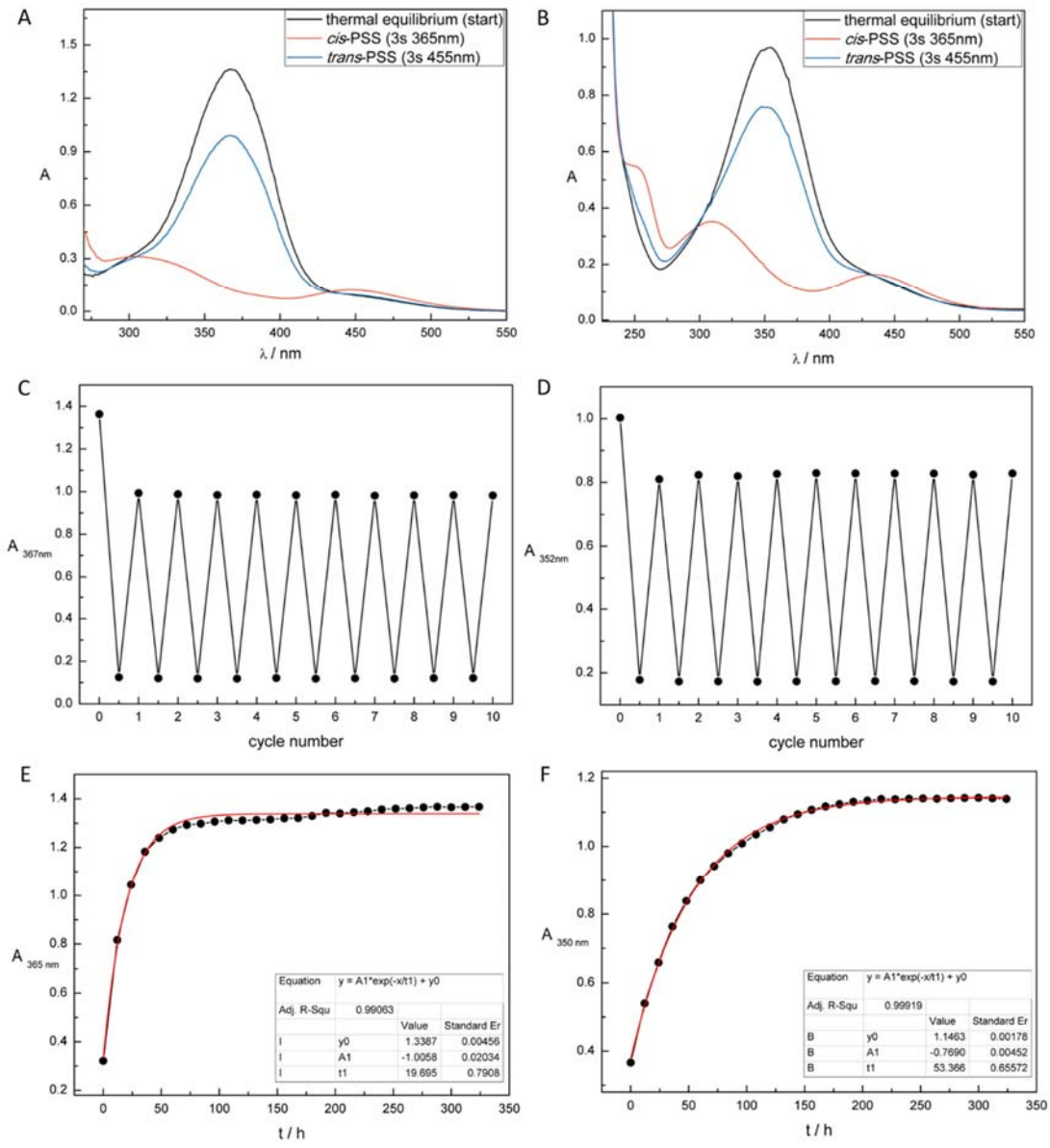

Figure S11. **Changes in absorption spectra of 42 upon continuous irradiation until the PSS is reached.** (A) 50 µM in DMSO. λ (*cis*-PSS) = 365 nm, λ (*trans*-PSS) = 455 nm. (B) 50 µM in phosphate buffer + 0.1% DMSO. λ (*cis*-PSS) = 365 nm, λ (*trans*-PSS) = 455 nm. **Cycle performance of 42.** (C) 50 µM in DMSO. Changes in absorption at 367 nm (λ_{max} of the *trans*-isomer) were measured during alternate irradiation with light of λ = 365 nm and λ = 455 nm until the PSS is reached. (D) 50 µM in phosphate buffer + 1% DMSO. Changes in absorption at 352 nm (λ_{max} of the *trans*-isomer) were measured during alternate irradiation with light of λ = 365 nm and λ = 455 nm until the PSS is reached. **Thermal stability of the *cis*-isomer of KR42 measured at 25 °C**. Black dots represent the absorption at the indicated wavelength dependent on the time of relaxation [h]. Red curve represents an exponential nonlinear curve fit. (E) 50 µM in DMSO. Changes in absorption maxima measured at 367 nm (λ_{max} of the *trans*-isomer) after irradiation with λ = 365 nm until the PSS is reached. $t_{0.5}$ = 13.6 h. (F) 50 µM solution in phosphate buffer + 1% DMSO. Changes in absorption maxima measured at 350 nm after irradiation with λ = 365 nm until the PSS is reached. $t_{0.5}$ = 37.0 h.

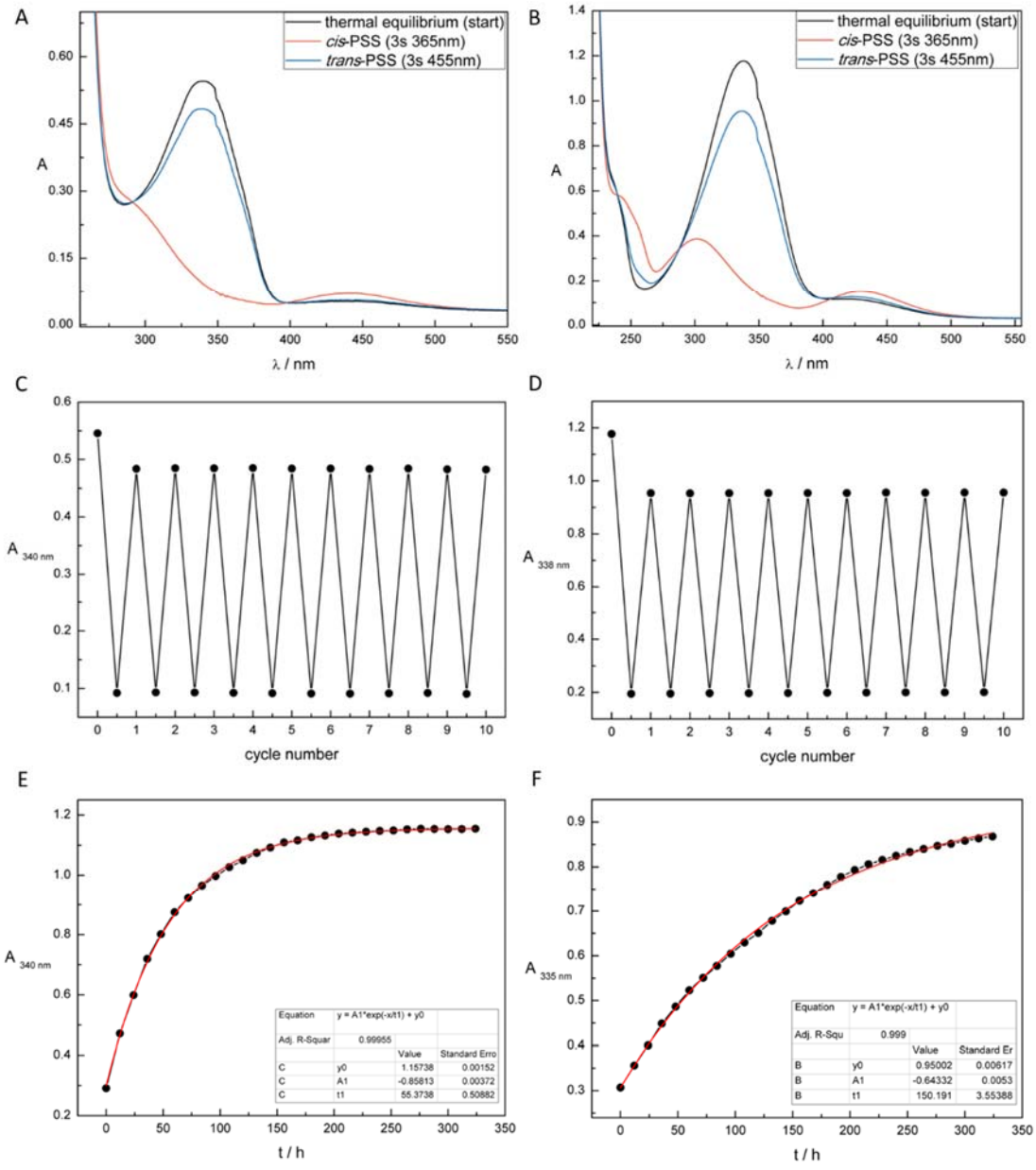

Figure S12. **Changes in absorption spectra of 49 upon continuous irradiation until the PSS is reached.** (A) 50 µM in DMSO. λ (*cis*-PSS) = 365 nm, λ (*trans*-PSS) = 455 nm. (B) 50 µM in phosphate buffer + 0.1% DMSO. λ (*cis*-PSS) = 365 nm, λ (*trans*-PSS) = 455 nm. **Cycle performance of 49.** (C) 50 µM in DMSO. Changes in absorption at 340 nm (λ_{max} of the *trans*-isomer) were measured during alternate irradiation with light of λ = 365 nm and λ = 455 nm until the PSS is reached. (D) 50 µM in phosphate buffer + 0.1% DMSO. Changes in absorption at 338 nm (λ_{max} of the *trans*-isomer) were measured during alternate irradiation with light of λ = 365 nm and λ = 455 nm until the PSS is reached. **Thermal stability of the *cis*-isomer of 49 measured at 25 °C**. Black dots represent the absorption at the indicated wavelength dependent on the time of relaxation [h]. Red curve represents an exponential nonlinear curve fit. (E) 50 µM in DMSO. Changes in absorption maxima measured at 340 nm (λ_{max} of the *trans*-isomer) after irradiation with λ = 365 nm until the PSS is reached. $t_{0.5}$ = 38.4 h. (F) 50 µM solution in phosphate buffer + 0.1% DMSO. Changes in absorption maxima measured at 335 nm after irradiation with λ = 365 nm until the PSS is reached. $t_{0.5}$ = 104 h.

Table S1. Photochemical properties of azobenzene-based galactosidase inhibitors measured 50 µM in DMSO at 25 °C.

Entry	Compound	λ_{max} *trans*-isomer [nm]	λ_{max} *cis*-isomer [nm]	Isosbestic points [nm]	Fatigue resistance	λ *trans*→*cis* [nm]	λ *cis*→*trans* [nm]
1	**4**	329	435	283, 386	excellent	365	455
2	**6**	401	445	271, 300, 360, 477	excellent	400	505
3	**34**	329	441	279, 389	excellent	365	455
4	**35**	331	436	282, 389	excellent	365	455
5	**36**	337	442	289, 396	excellent	365	455
6	**37**	327	440	278, 394	excellent	365	455
7	**38**	328	432	278, 386	excellent	365	455
8	**39**	336	446	288, 399	excellent	365	455
9	**40**	322	-	-	excellent	385	470
10	**41**	363	440	283, 426	excellent	385	455
11	**42**	367	446	302, 433	excellent	365	455
12	**49**	340	441	291, 398	excellent	365	455

Table S2. Photochemical properties of azobenzene-based galactosidase inhibitors measured 50 µM in phosphate buffer + 0.01% DMSO, and 1% DMSO*, respectively.

Entry	Compound	λ_{max} *trans*-isomer [nm]	λ_{max} *cis*-isomer [nm]	Isosbestic points [nm]	Fatigue resistance	λ *trans*→*cis* [nm]	λ *cis*→*trans* [nm]
1	**4**	323	425	237, 280, 385	excellent	365	455
2	**6**	379	-	279, 293, 335, 464	excellent	455	-
3	**34**	325	431	234, 274, 390	excellent	365	455
4	**35**	329	426	238, 278, 396	excellent	365	455
5	**36***	334	431	242, 287, 399	excellent	365	455
6	**37**	325	431	241, 275, 390	excellent	365	455
7	**38**	323	423	235, 273, 388	excellent	365	455
8	**39***	335	434	245, 288, 399	excellent	365	455
9	**40**	322	428	235, 254, 273, 428	excellent	365	455
10	**41**	348	429	238, 280, 421	excellent	365	455
11	**42***	352	433	241, 297, 432	excellent	365	455
12	**49**	338	430	240, 288, 407	excellent	365	455

HPLC- and NMR-Based Photochromic Characterization.

Table S3. Distribution of both isomers at their photostationary states [%]. Irradiation wavelengths indicated in brackets. Thermal half-lives [h] determined by UV-Vis absorption spectroscopy at rt after irradiation with the indicated wavelengths to accumulate a substantial amount of the *cis*-isomer.

Entry	Cpd	PSS-distribution (DMSO)	PSS-distribution (aqueous media)	THL [h] (DMSO)	THL [h] (PBS+0.1% / 1%* DMSO)
1	**4**	74% *cis* (375 nm) [a] 88% *trans* (405 nm) [a]	67% *cis* (375 nm) [a] 75% *trans* (405 nm) [a]	121	536
2	**6**	91% *cis* (400 nm) [b] 64% *trans* (505 nm) [b]	n.d.	3.53	$4.70 \cdot 10^{-4}$
3	**34**	53% *cis* (365 nm) [b] 78% *trans* (455 nm) [b]	93% *cis* (365 nm) [b] 74% *trans* (455 nm) [b]	84.4	98.2
4	**35**	93% *cis* (365 nm) [a] 82% *trans* (455 nm) [a]	88% *cis* (365 nm) [a] 72% *trans* (455 nm) [a]	80.2	252
5	**36***	63% *cis* (365 nm) [b] 72% *trans* (455 nm) [b]	90% *cis* (365 nm) [b] 82% *trans* (455 nm) [b]	65.2	131
6	**37**	86% *cis* (365 nm) [b] 83% *trans* (455 nm) [b]	76% *cis* (365 nm) [b] 77% *trans* (455 nm) [b]	122	17.4
7	**38**	89% *cis* (365 nm) [a] 81% *trans* (455 nm) [a]	83% *cis* (365 nm) [a] 75% *trans* (455 nm) [a]	106	203
8	**39***	92% *cis* (365 nm) [b] 82% *trans* (455 nm) [b]	90% *cis* (365 nm) [b] 82% *trans* (455 nm) [b]	27.2	25.3
9	**40**	84% *cis* (385 nm) [a] 63% *trans* (455 nm) [a]	81% *cis* (365 nm) [a] 63% *trans* (455 nm) [a]	56.2	262
10	**41**	91% *cis* (385 nm) [a] 73% *trans* (455 nm) [a]	88% *cis* (365 nm) [a] 69% *trans* (455 nm) [a]	28.5	94.3
11	**42***	89% *cis* (365 nm) [a] 70% *trans* (455 nm) [a]	90% *cis* (365 nm) [a] 76% *trans* (455 nm) [a]	13.6	37.0
12	**49**	96% *cis* (365 nm) [a] 80% *trans* (455 nm) [a]	93% *cis* (365 nm) [a] 74% *trans* (455 nm) [a]	38.4	104

[a] determined by analytical HPLC measurement of a preirradiated 50 µM solution in DMSO and phosphate buffer + 0.1% DMSO, and 1% DMSO,* respectively, at 20 °C. [b] determined by NMR-measurement of a preirradiated solution in DMSO and D_2O + 5% DMSO,* respectively.

^{1}H- and ^{13}C-NMR spectra

Compound **4** (DMSO-d_6)

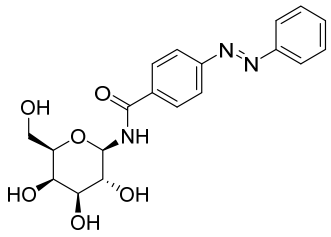

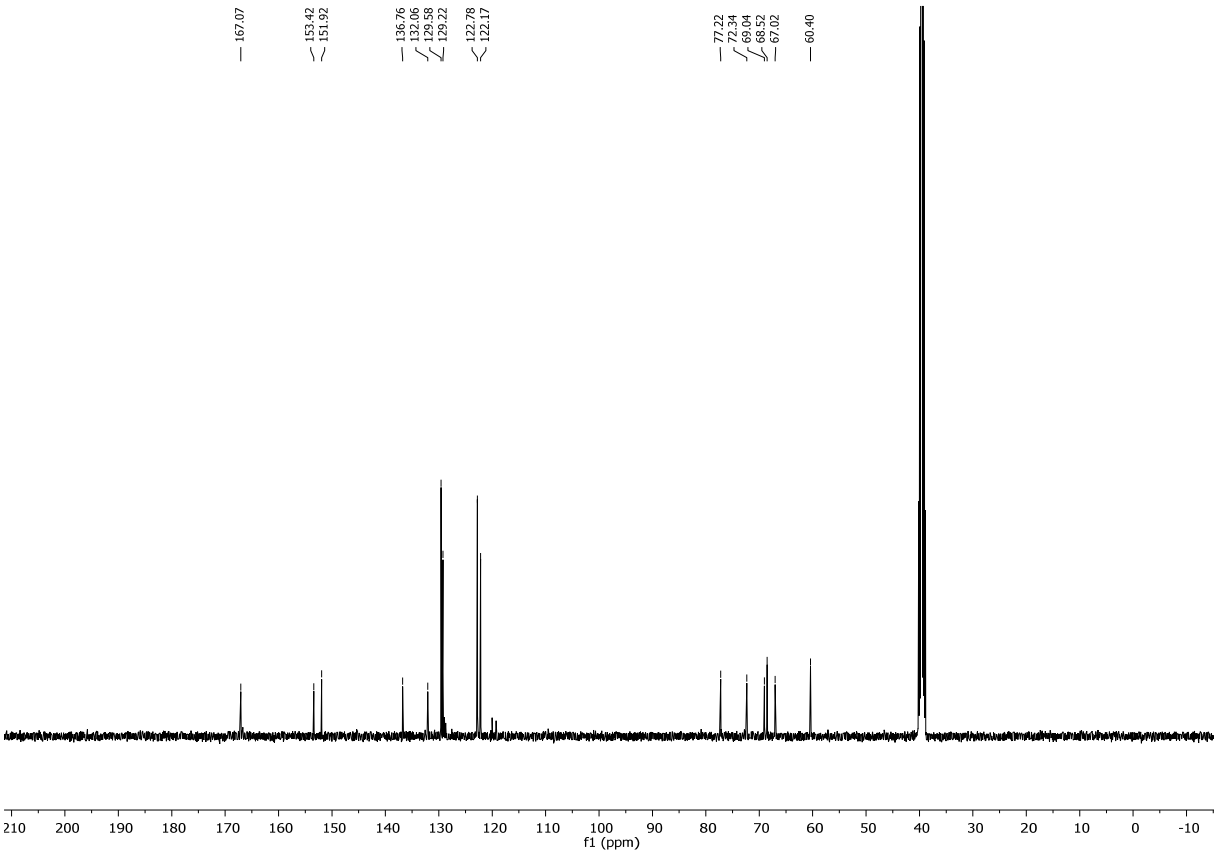

Compound **6** (DMSO-d_6)

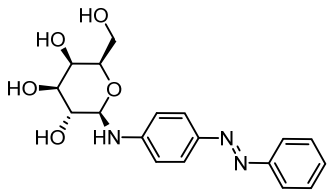

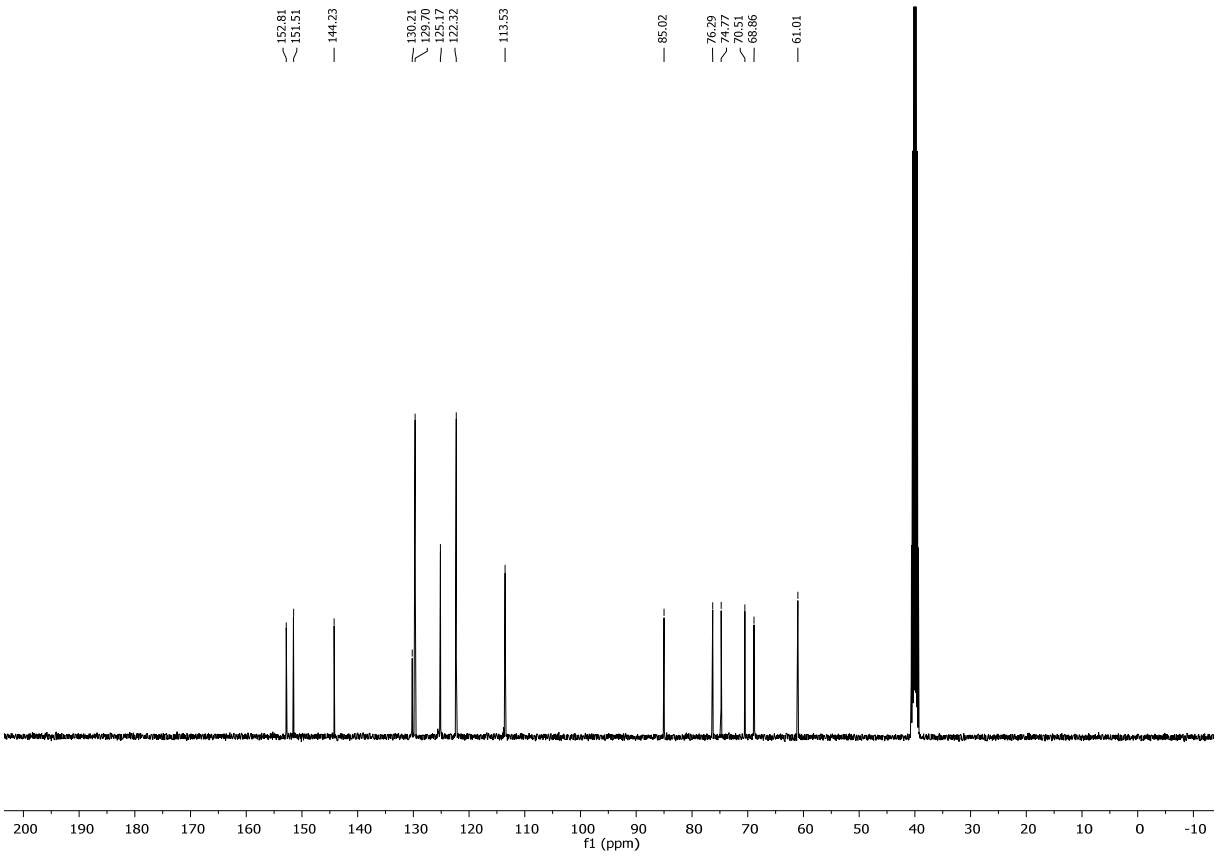

Compound **11** ($CDCl_3$-*d*)

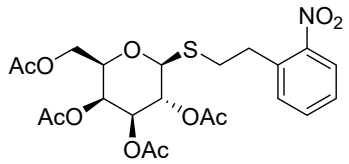

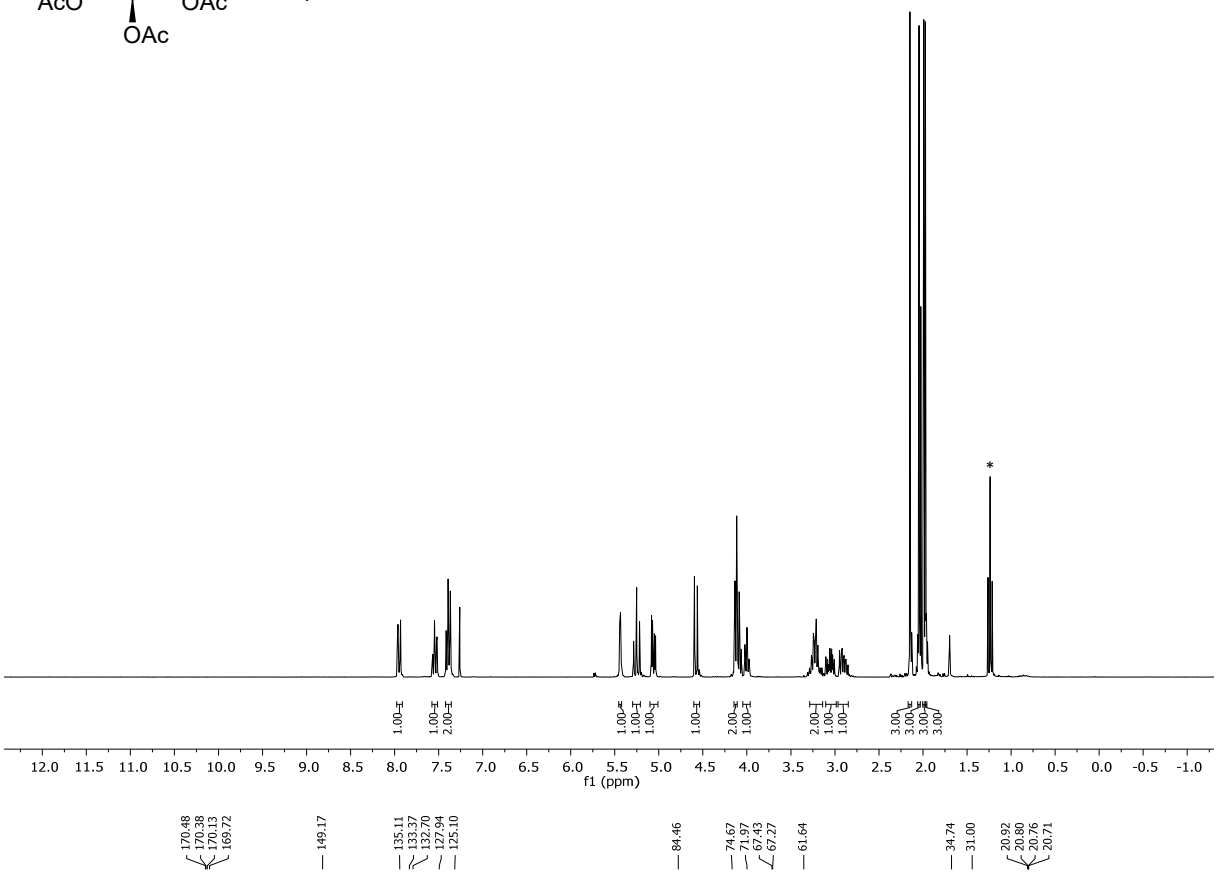

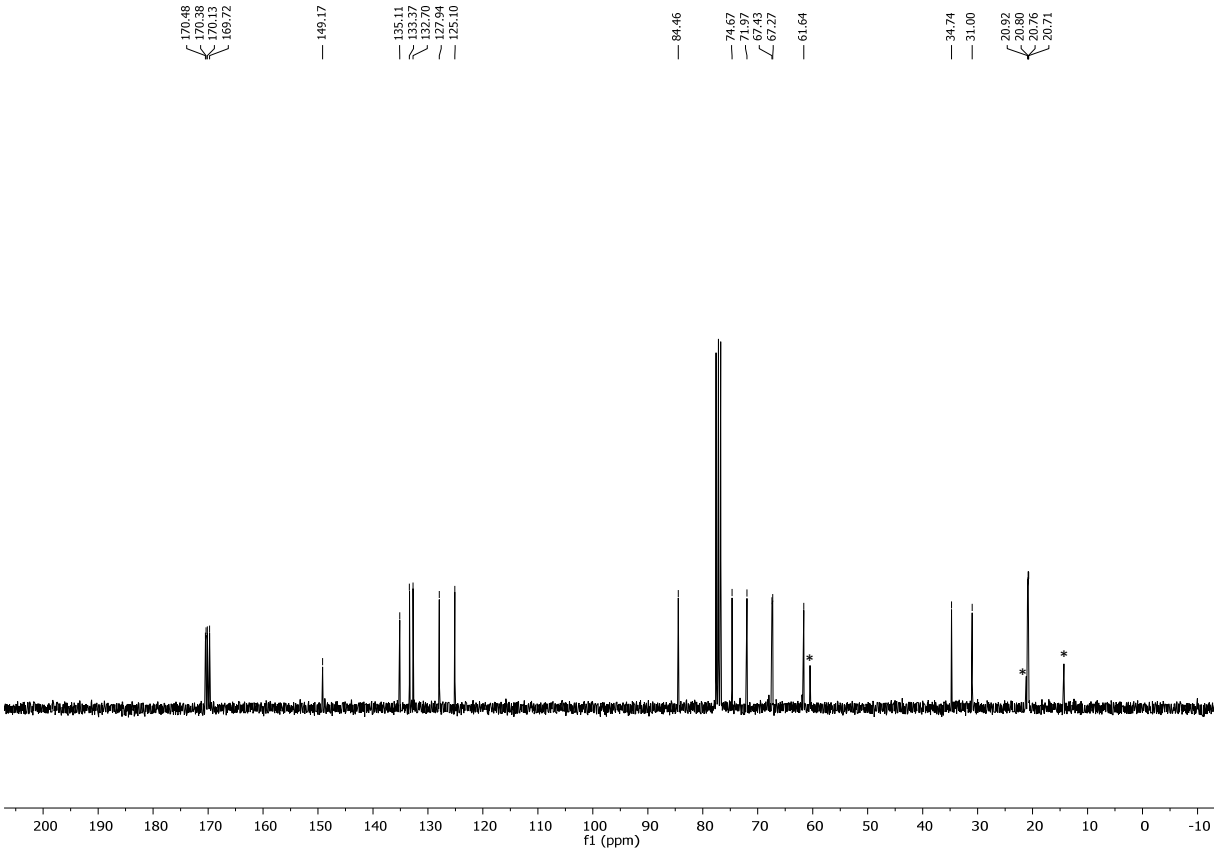

* solvent residual signal: ethyl acetate

Compound **12** ($CDCl_3$-*d*)

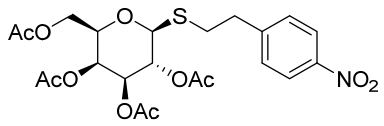

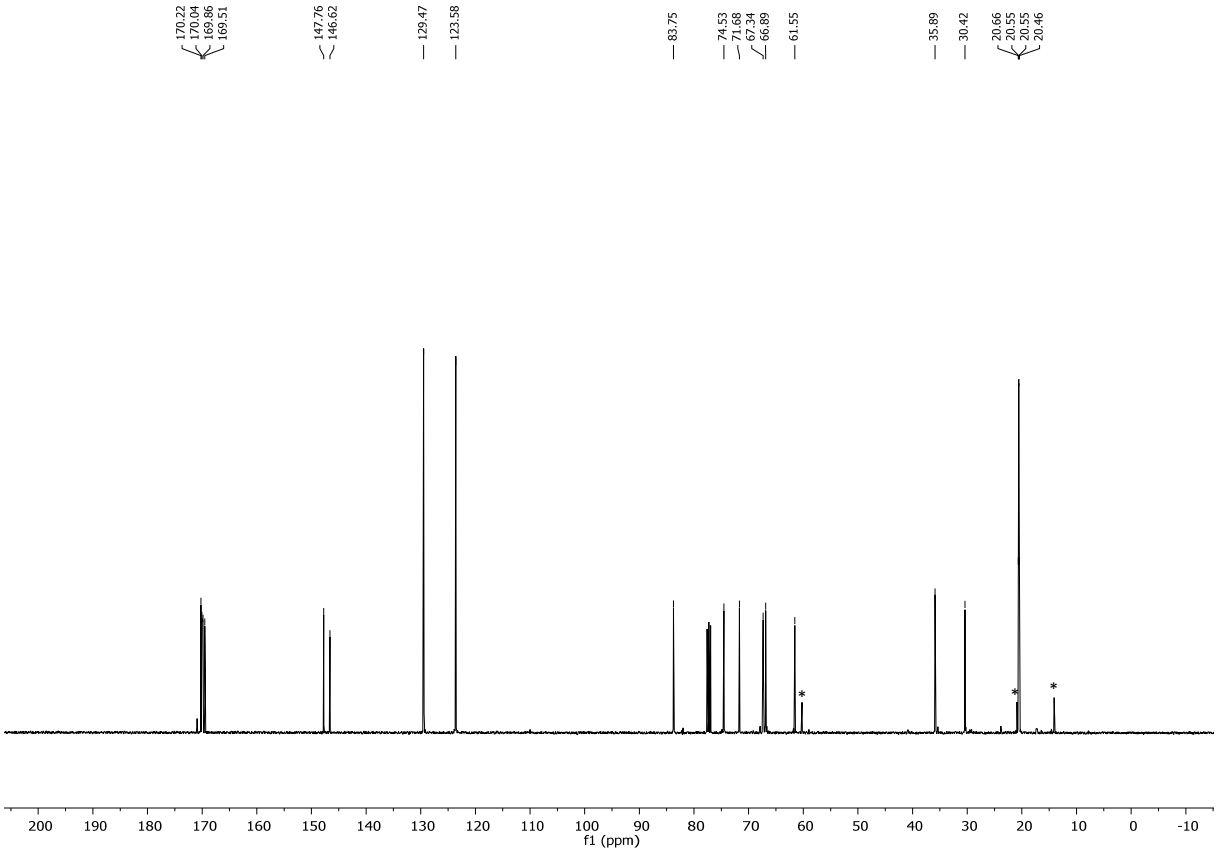

* solvent residual signal: ethyl acetate

Compound **13** ($CDCl_3$-*d*)

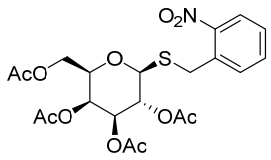

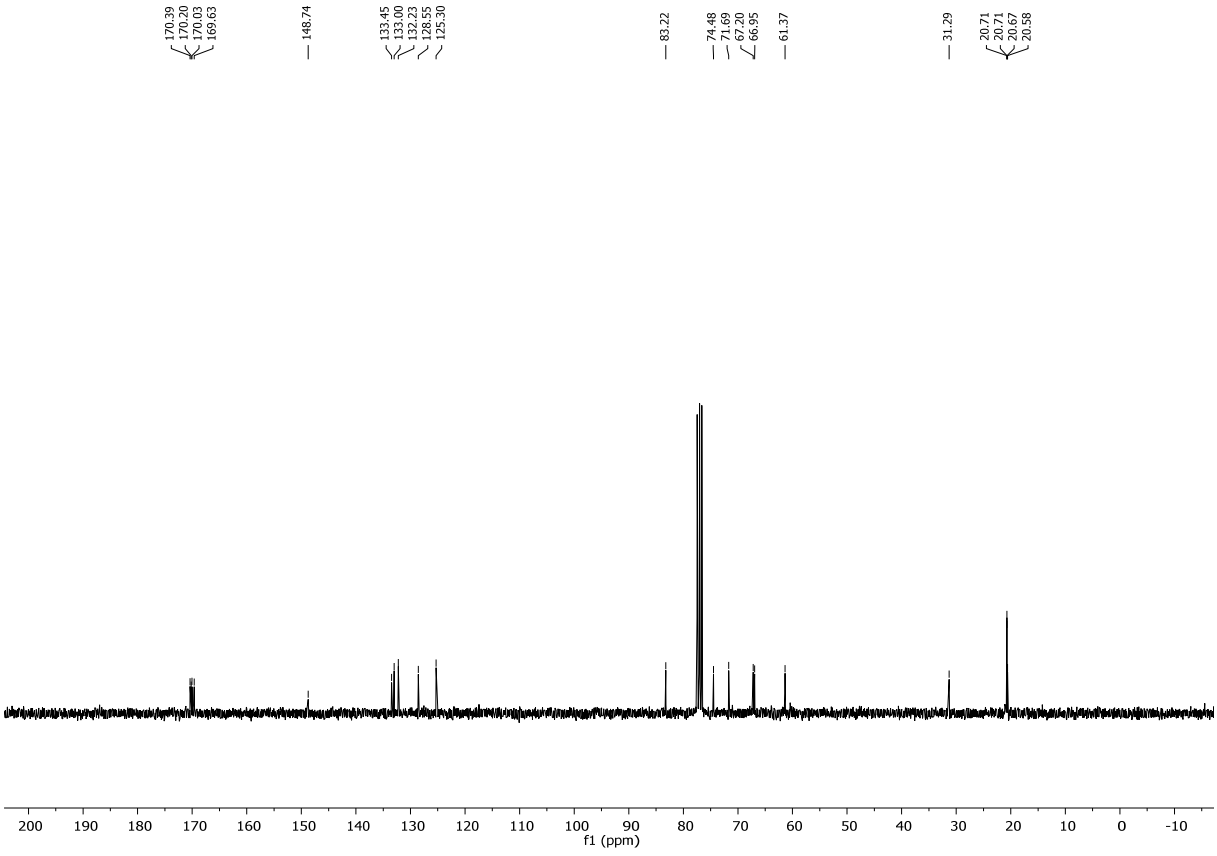

* solvent residual signal: ethyl acetate

Compound **14** ($CDCl_3$-*d*)

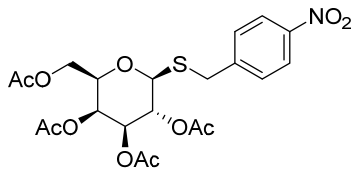

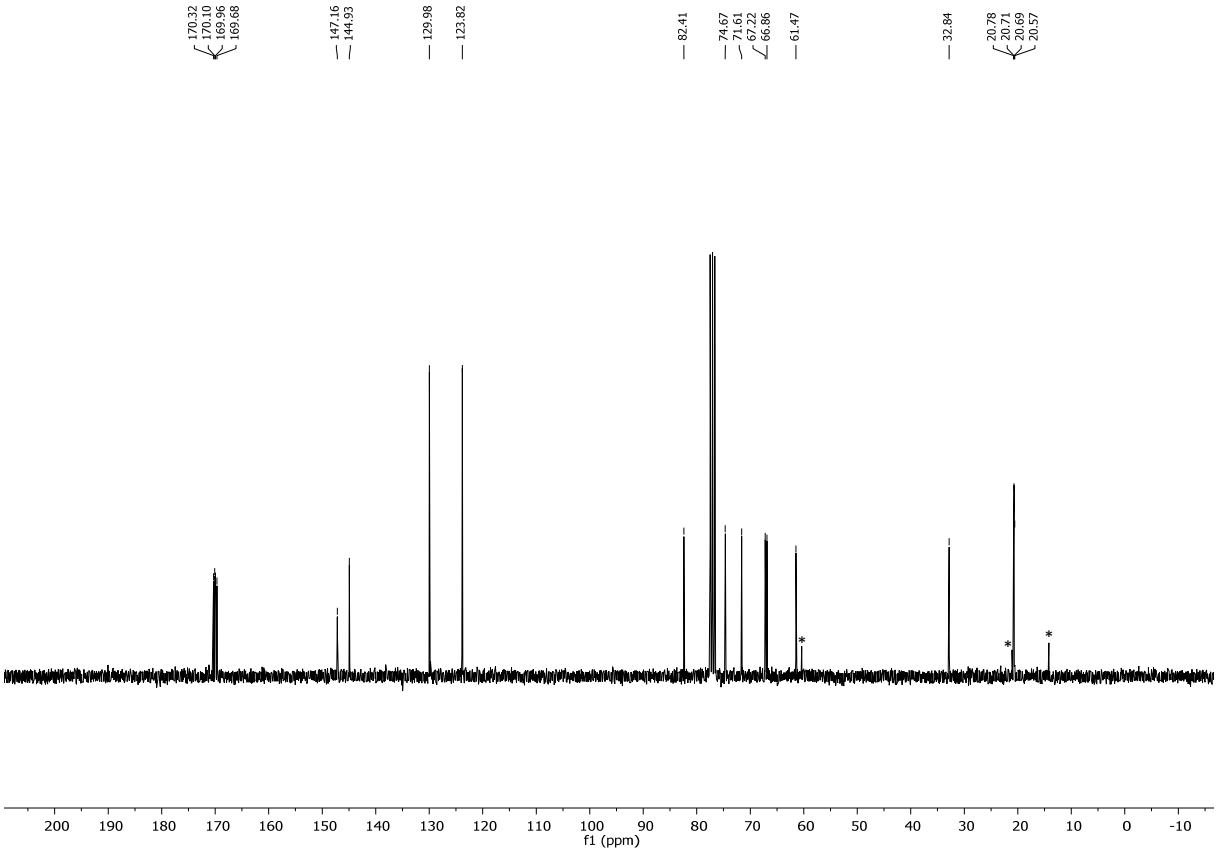

* solvent residual signal: ethyl acetate

Compound **15** ($CDCl_3$-*d*)

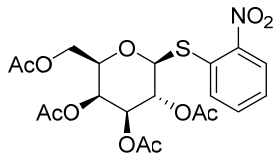

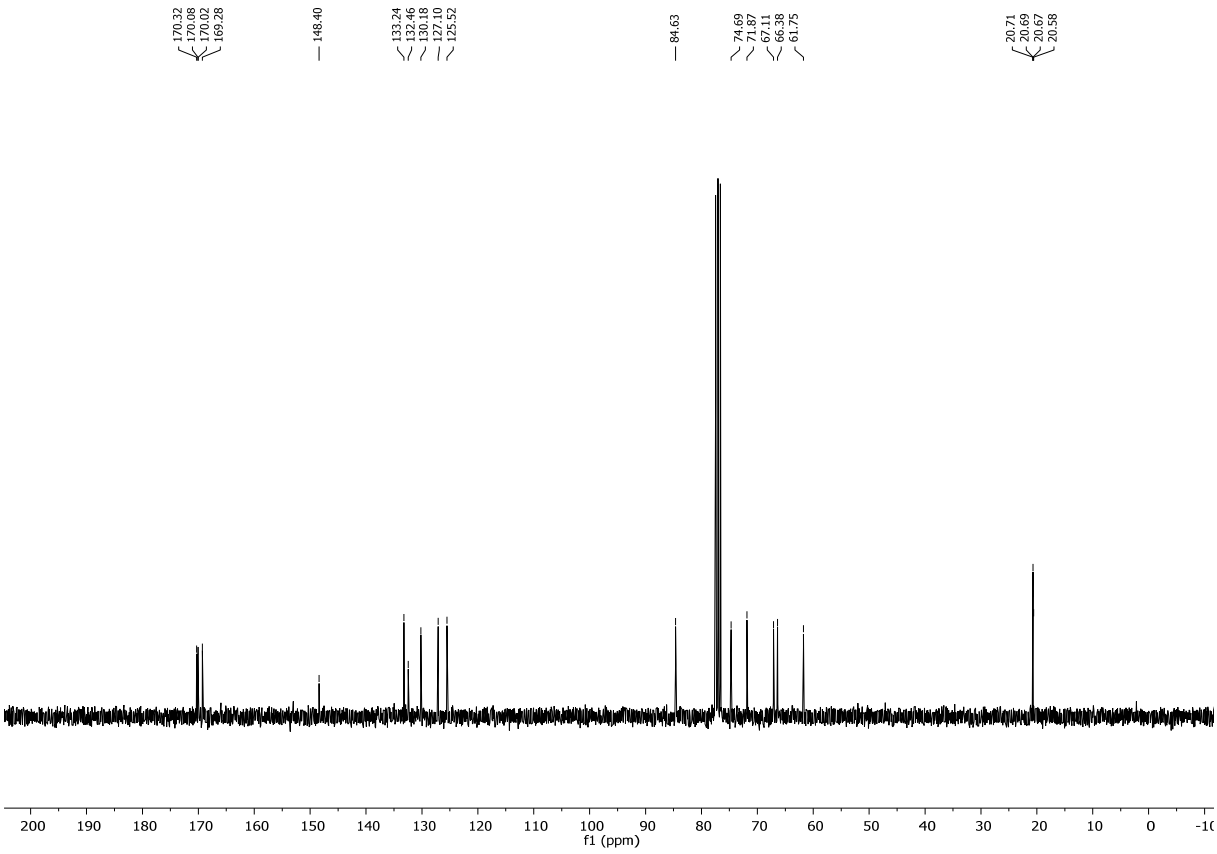

* solvent residual signal: ethyl acetate

Compound **16** (DMSO-d_6)

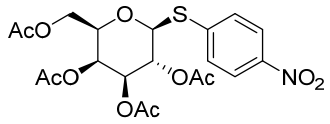

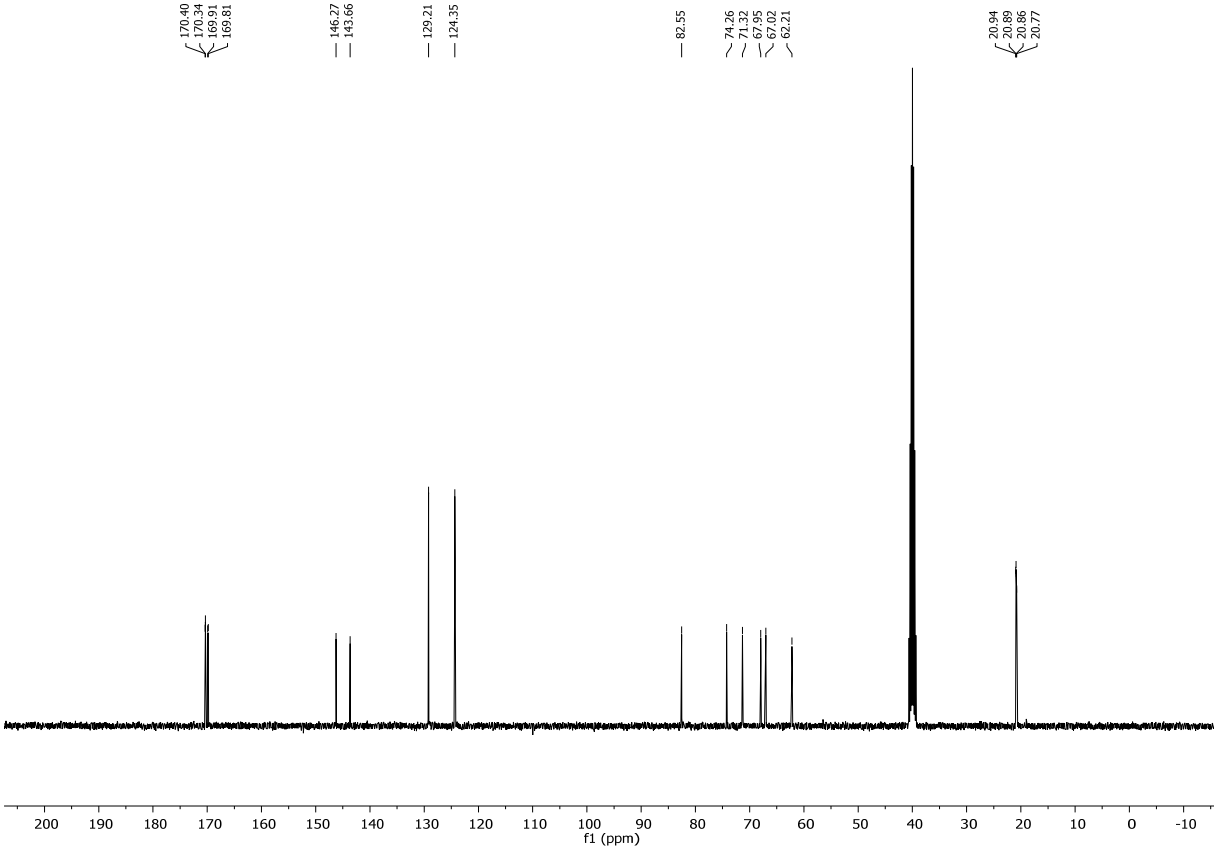

* solvent residual signal: ethyl acetate

Compound **34** (DMSO-d_6)

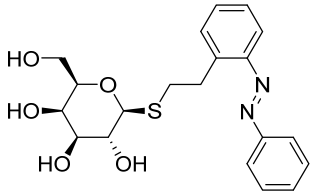

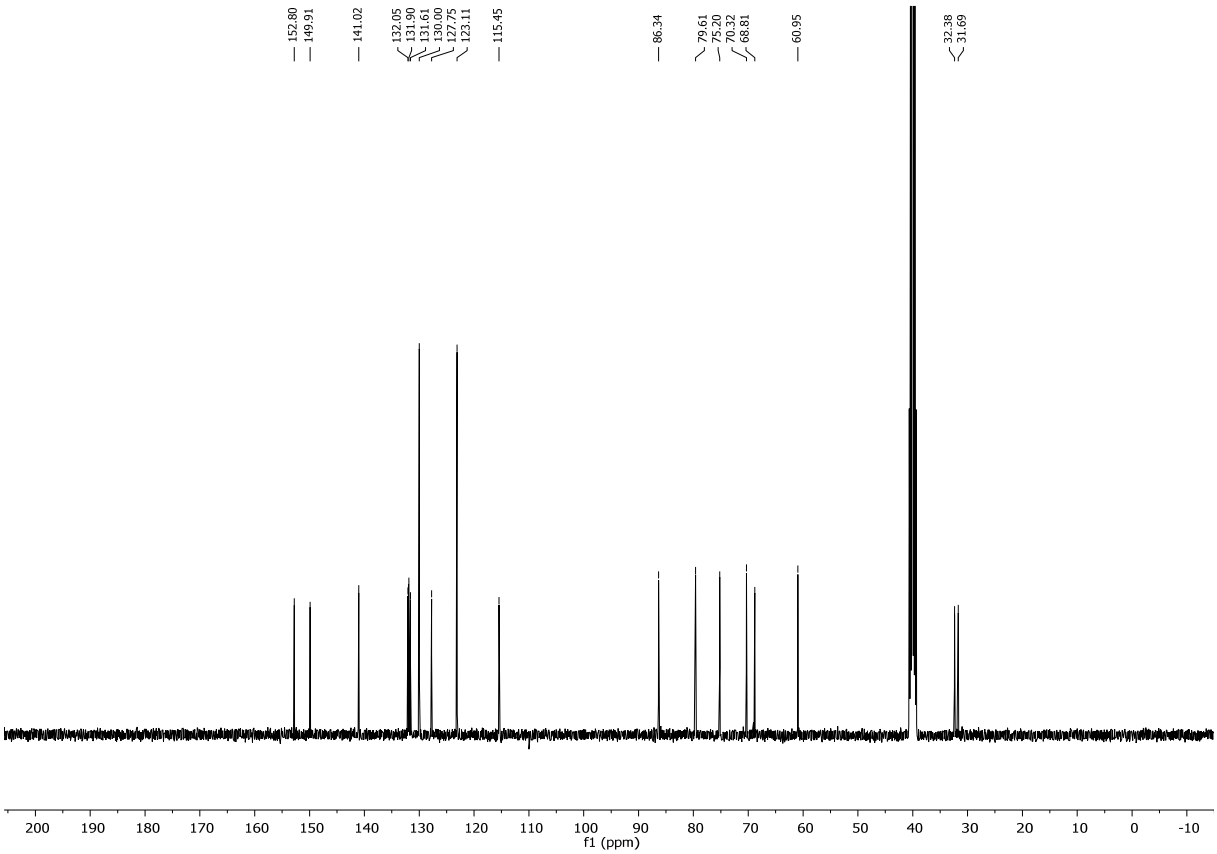

Compound **35** (DMSO-d_6)

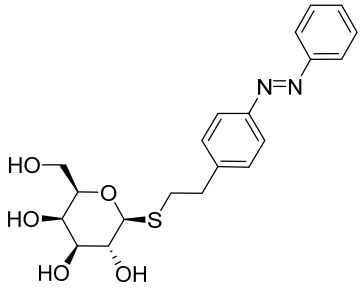

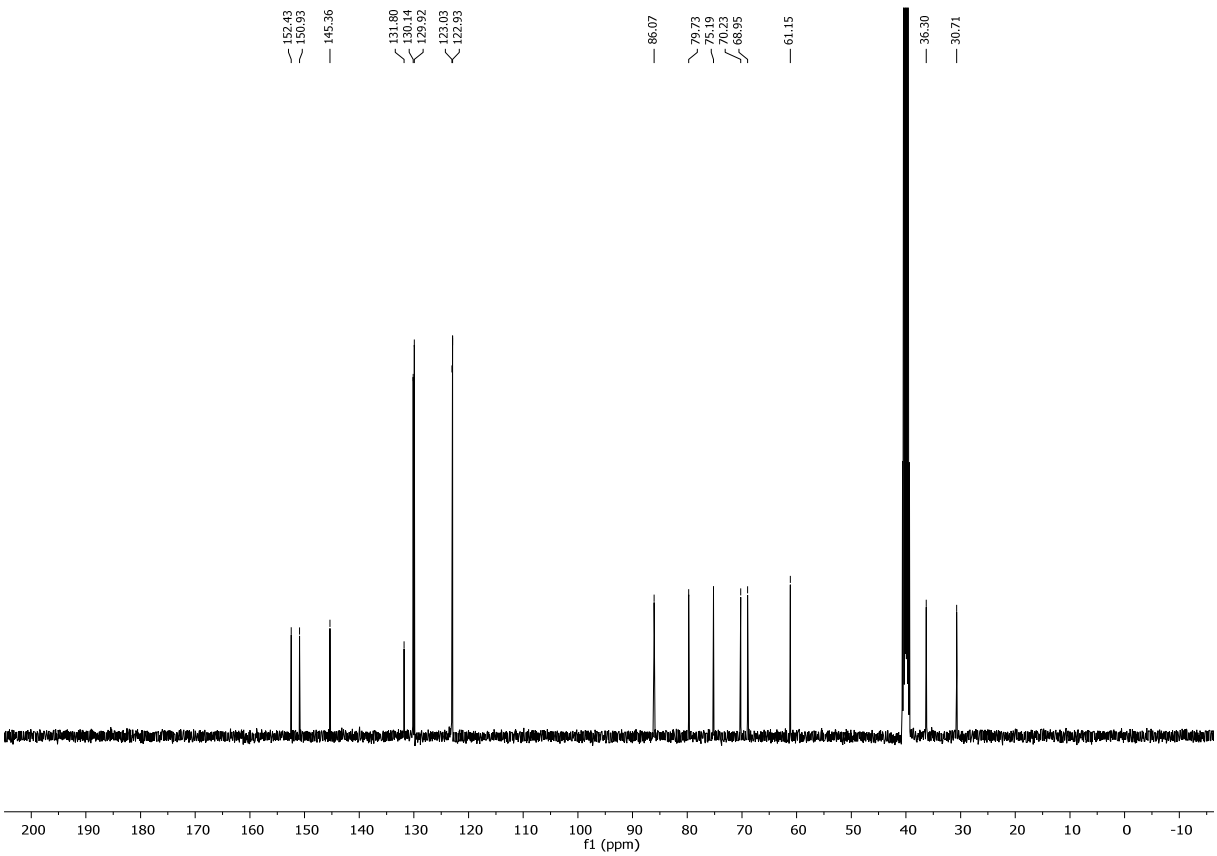

Compound **36** (DMSO-d_6)

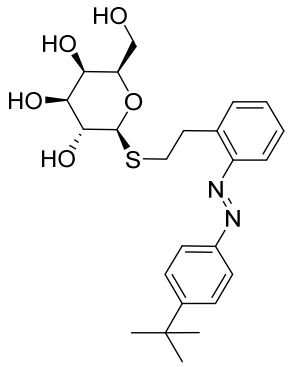

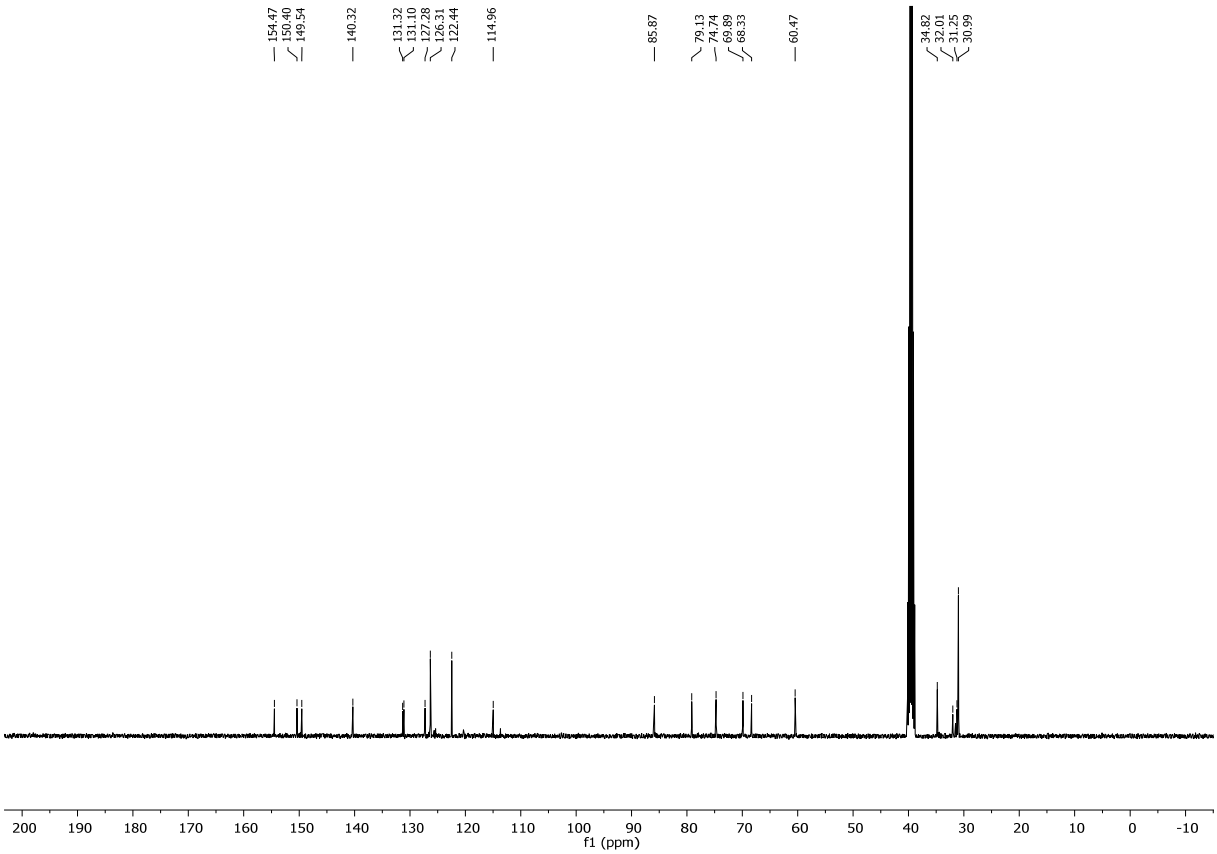

Compound **37** (DMSO-d_6)

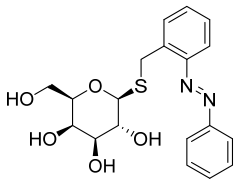

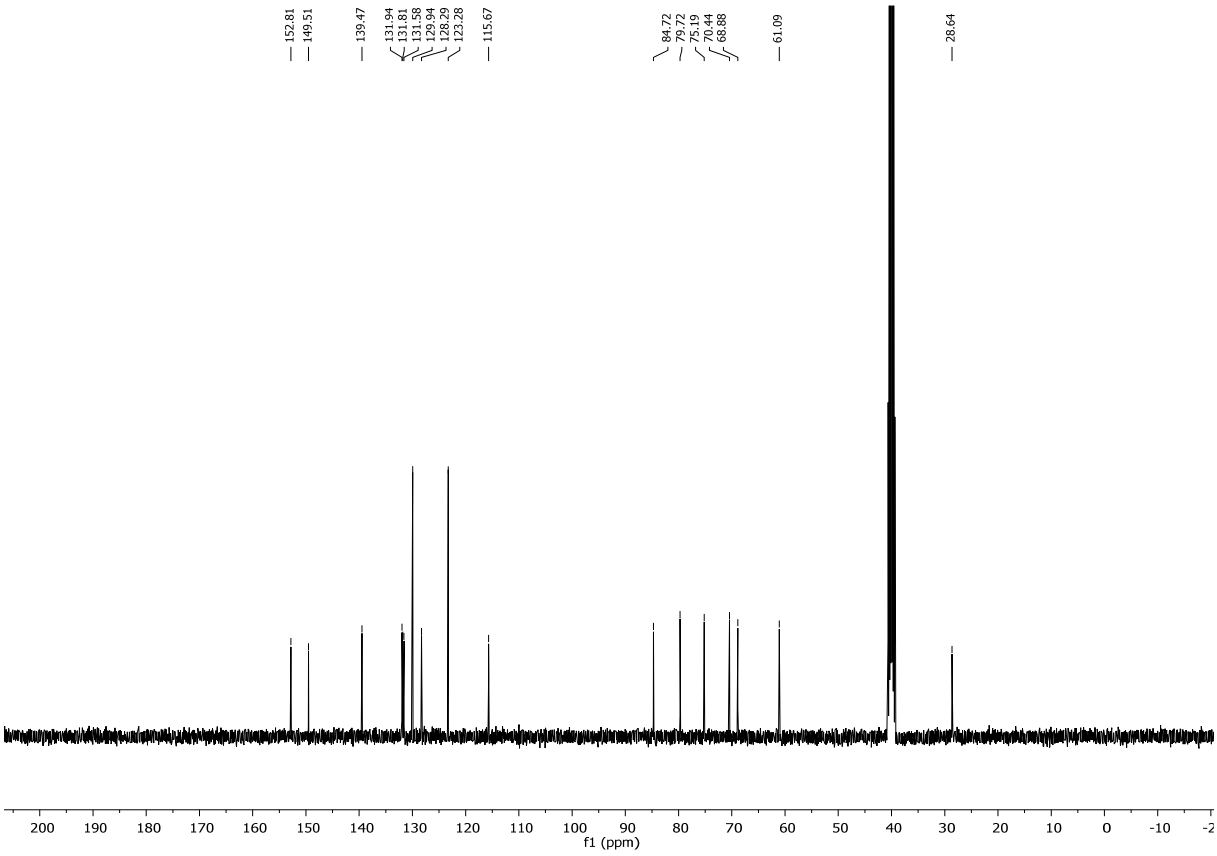

Compound **38** (DMSO-d_6)

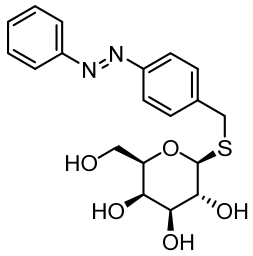

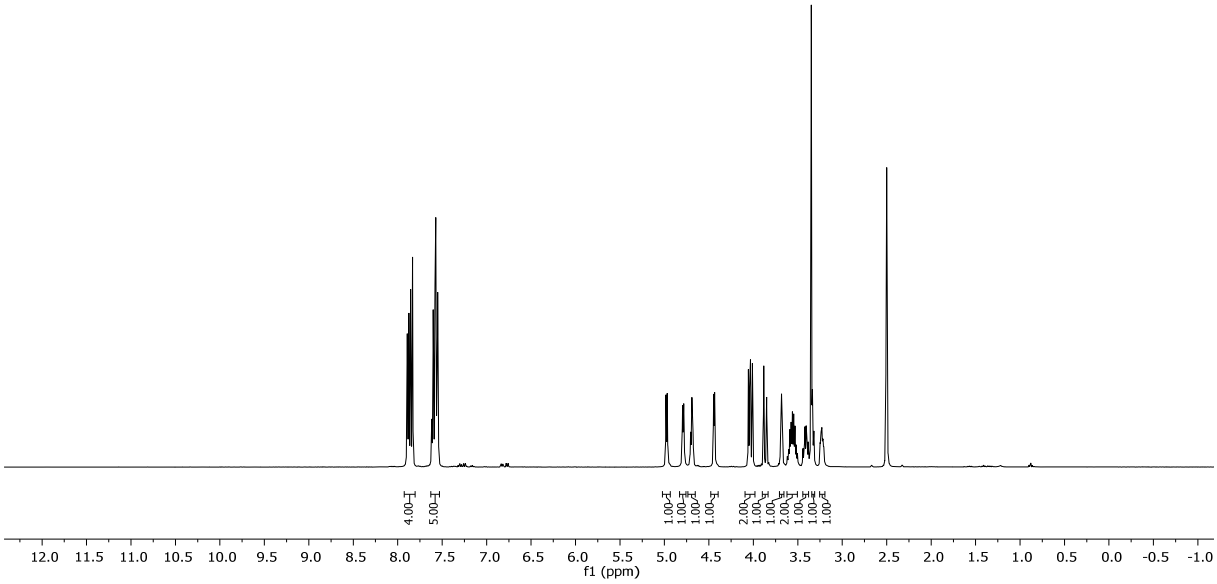

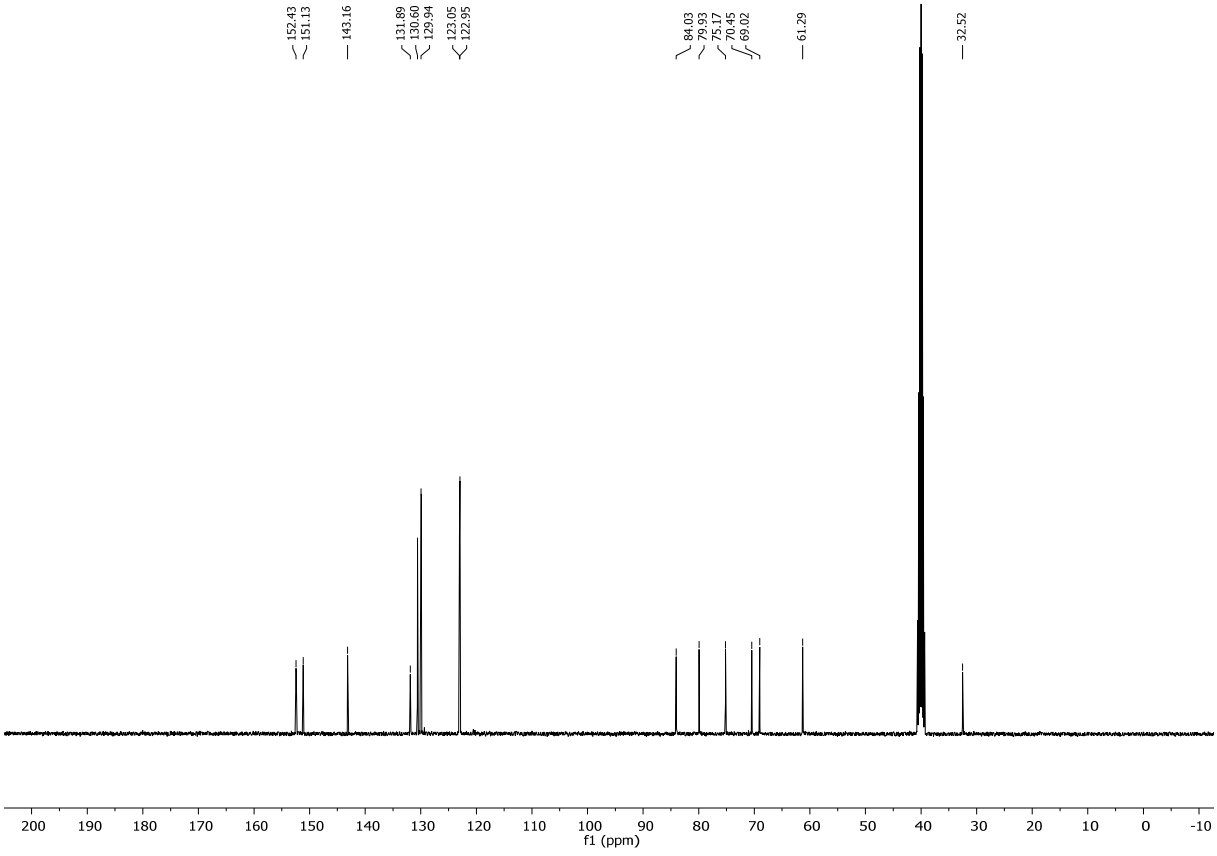

Compound **39** (DMSO-d_6)

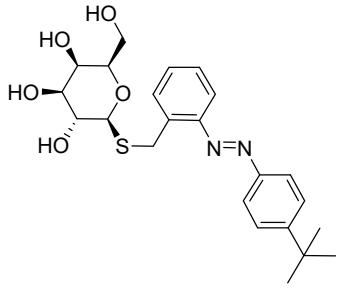

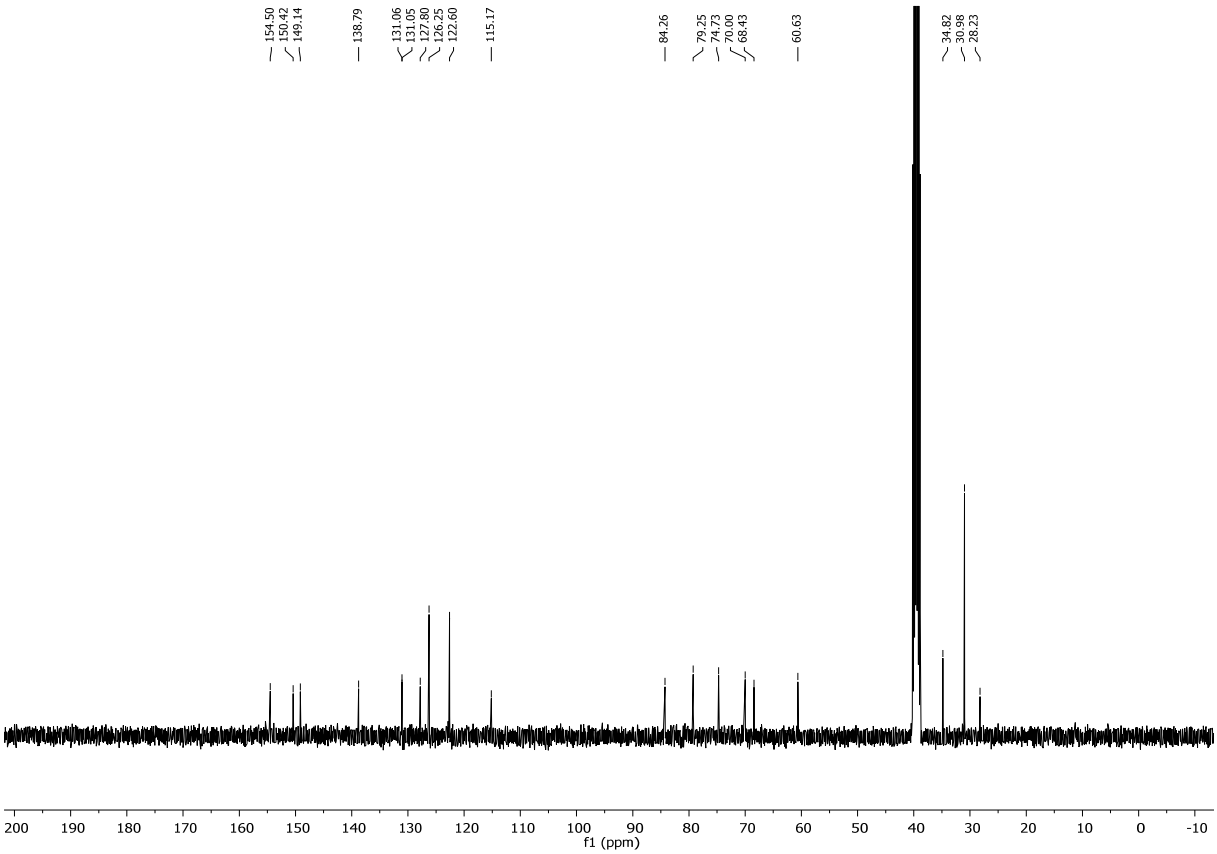

Compound **40** (DMSO-d_6)

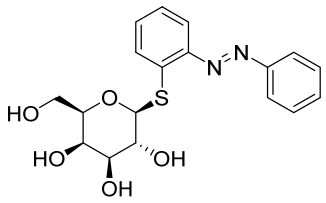

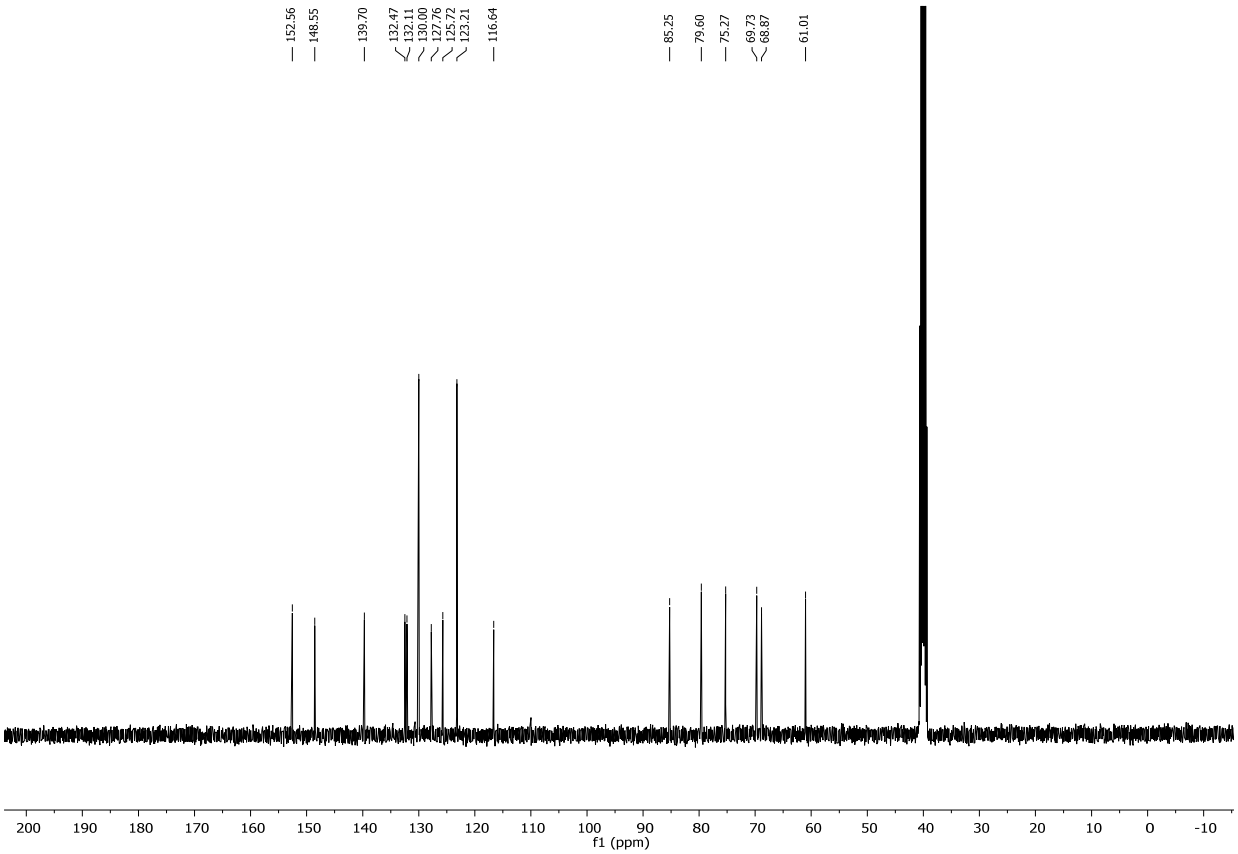

Compound **41** (DMSO-d_6)

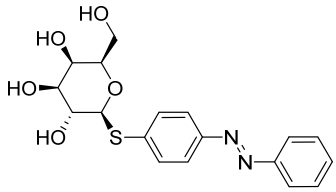

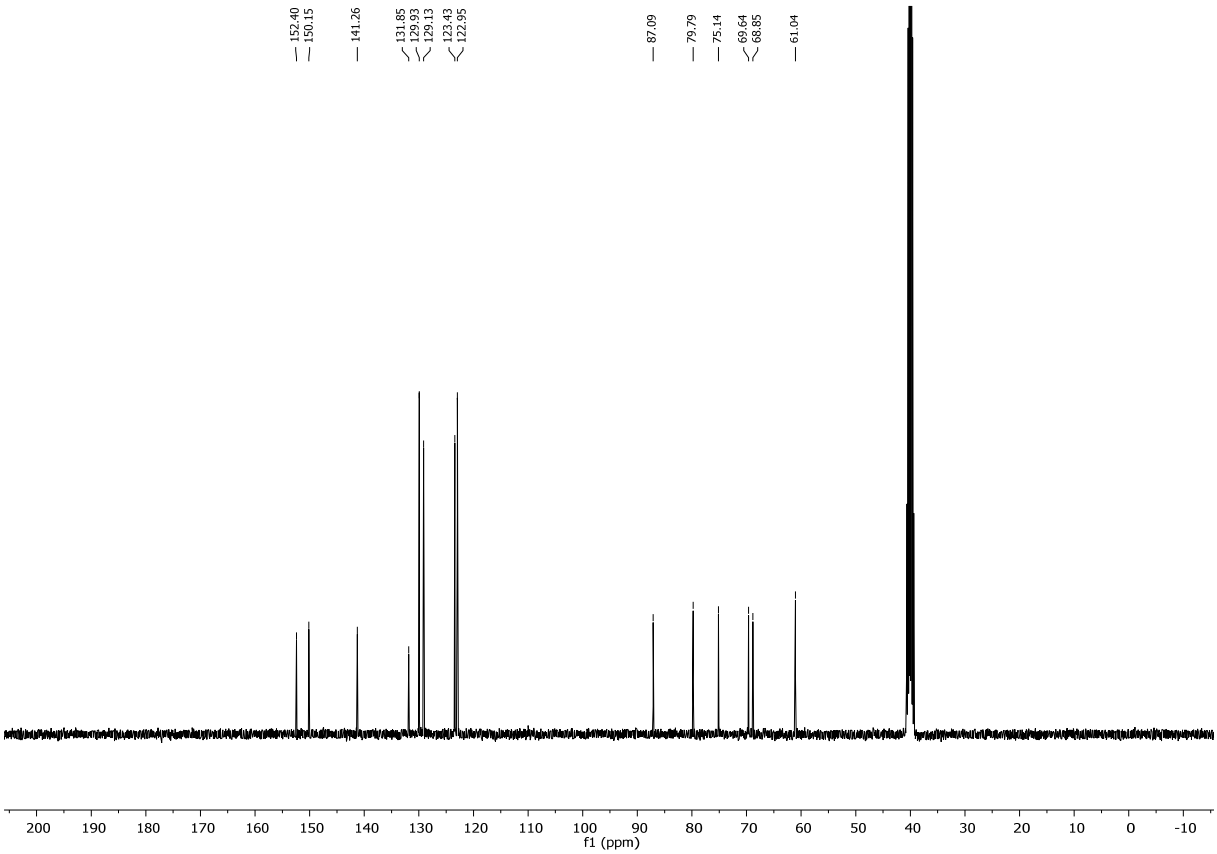

Compound **42** (DMSO-d_6)

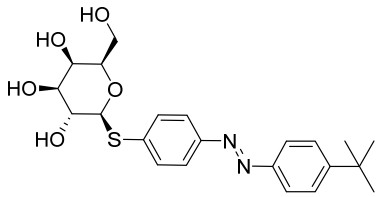

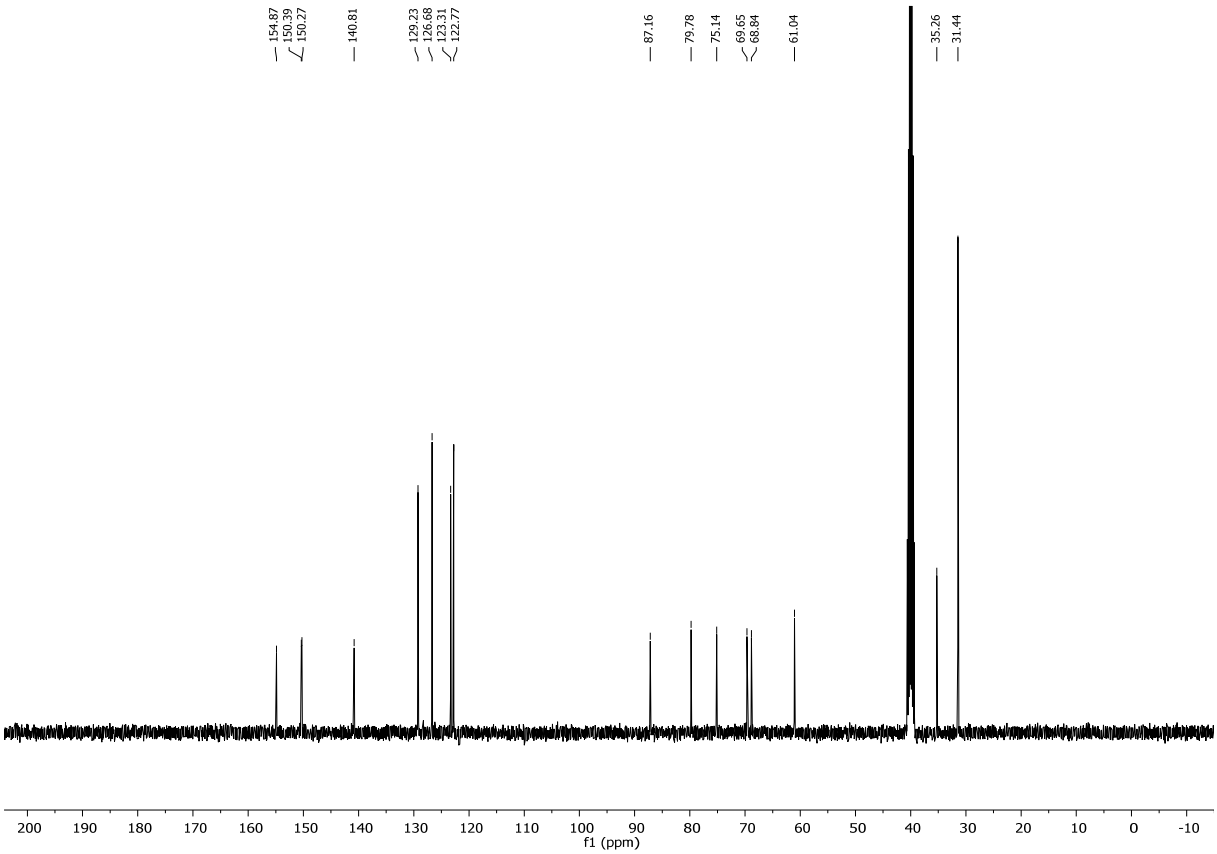

Compound **45** (DMSO-d_6)

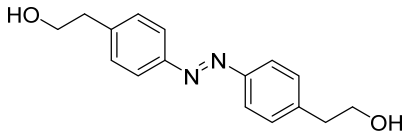

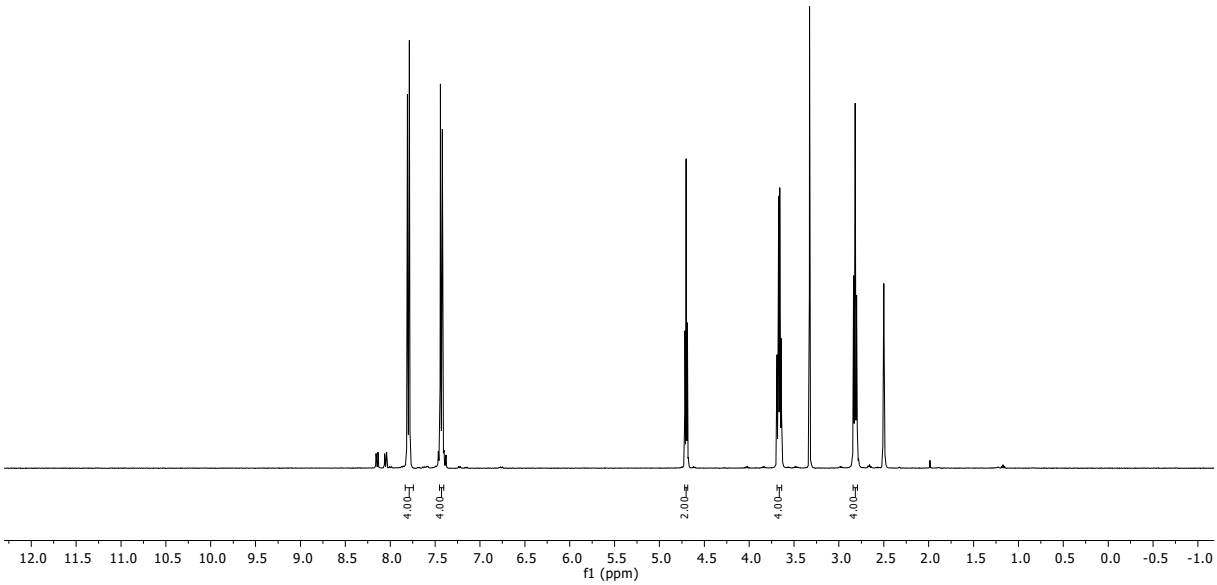

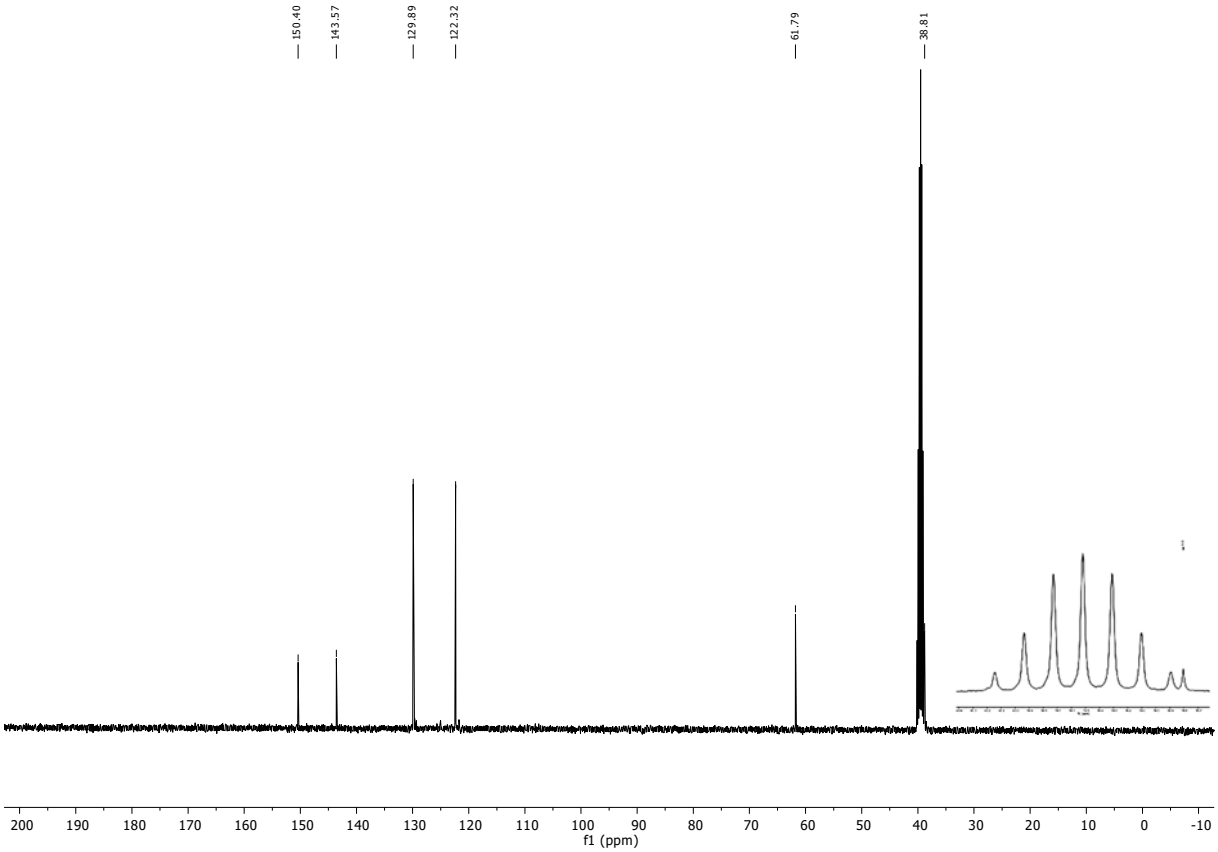

Compound **46** (DMSO-d_6)

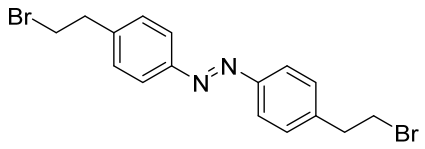

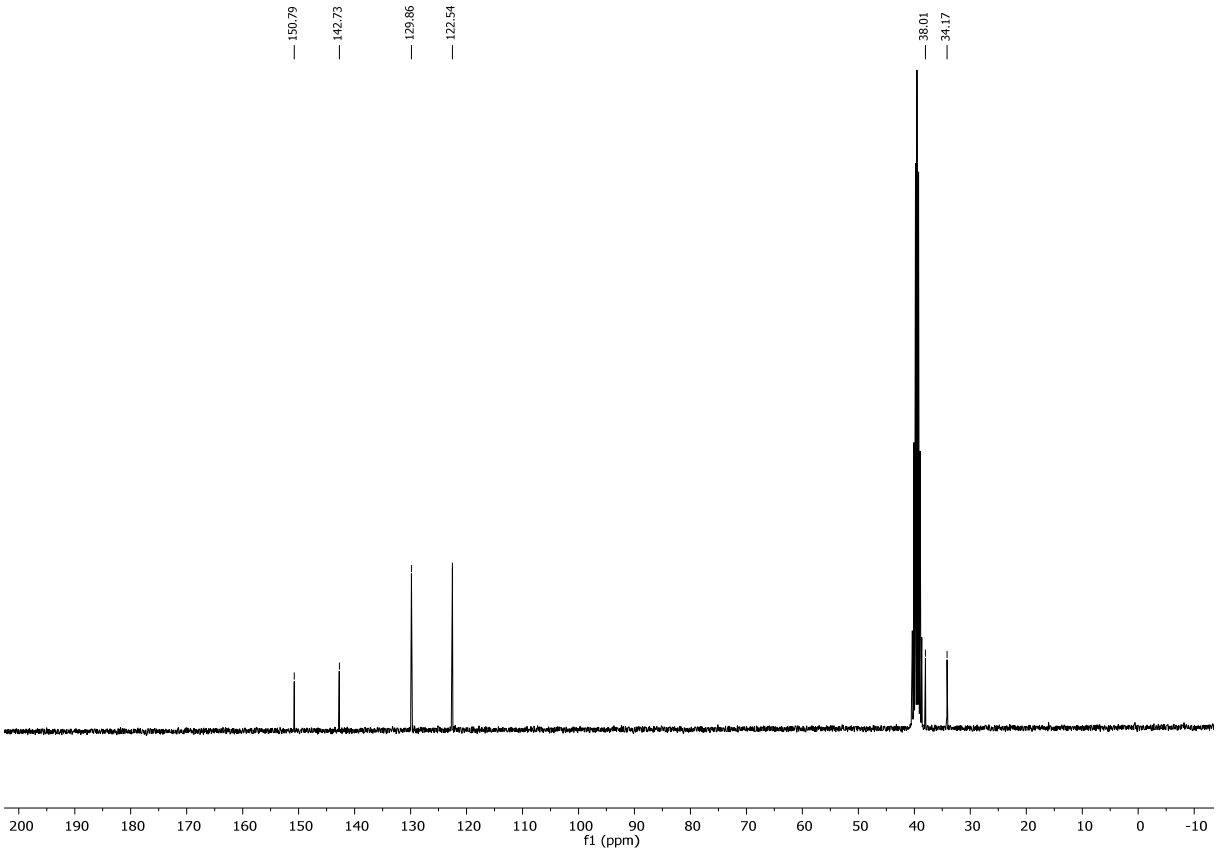

Compound **49** (DMSO-d_6)

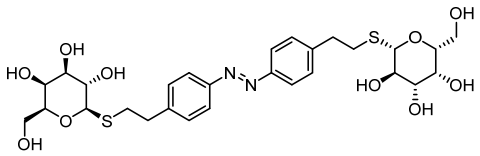

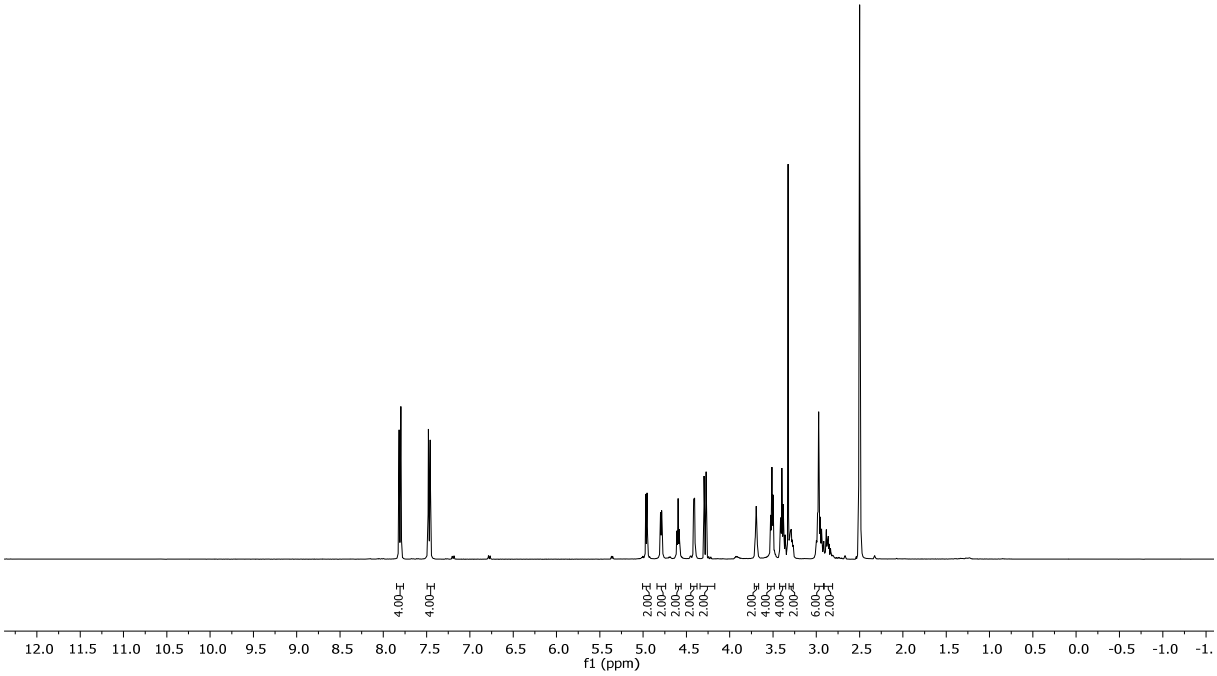

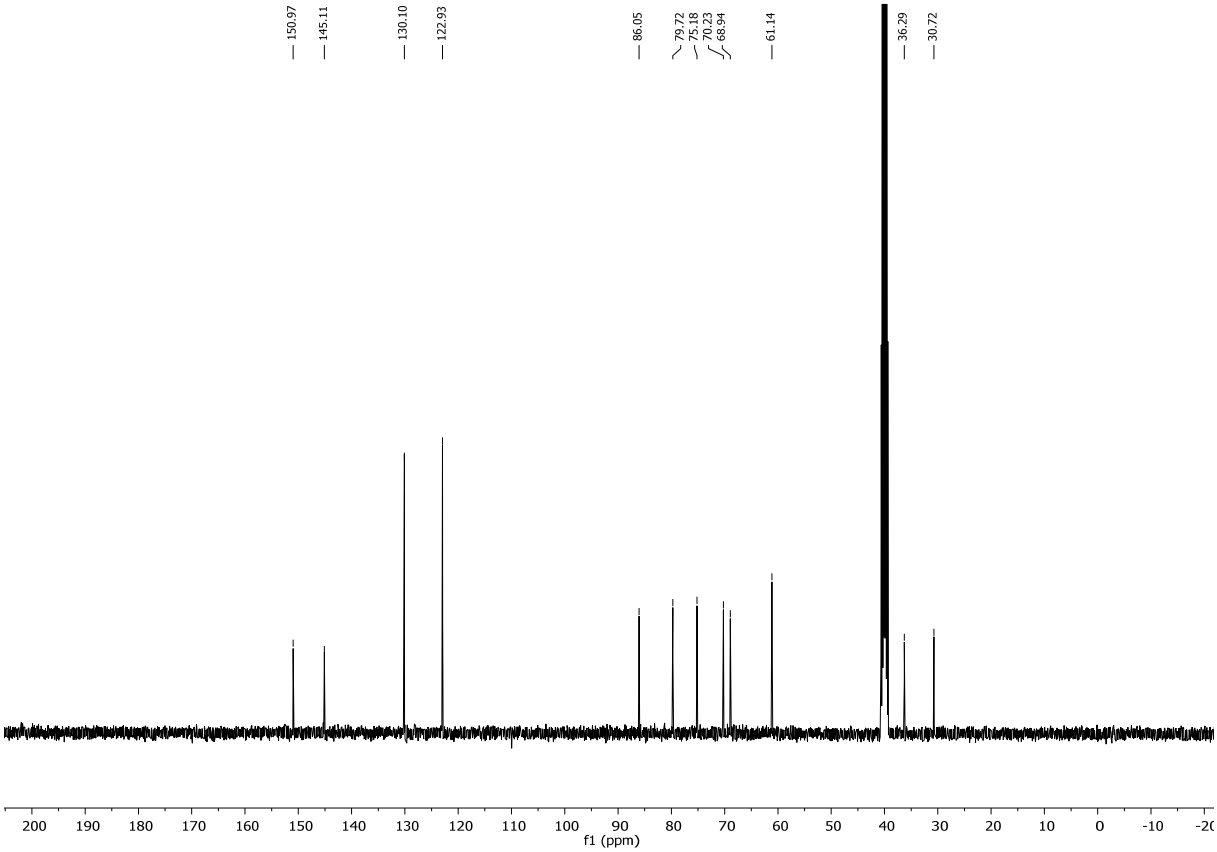

Enzymatic inhibition.

Table S4. Inhibitory activity of photochromic competitive β-galactosidase inhibitors measured at a substrate concentration of 100 µM, an enzyme concentration of 36 pM. Inhibitor concentrations were chosen according to the compound solubility and are indicated below.

Entry	Compound	relative activity *trans*-isomer [%]	relative activity *cis*-PSS [%]	Ratio (*cis*/*trans*)
1	**4**[b]	77±29	85±15	1.1
2	**6**[b,e]	78.5±1.7	n.d.[a]	-
3	**34**[b,e]	0.48±0.16	0.88±0.09	1.8
4	**35**[b,e]	16.6±1.6	11.8±2.1	0.7
5	**36**[d,e]	23.7±2.4	15.2±1.0	0.6
6	**37**[b]	-6.28±0.11	0.346±0.023	-
7	**38**[b]	23±3	22±4	1.0
8	**39**[d,e]	13.4±1.9	10.5±1.7	0.8
9	**40**[b]	18.9±1.2	23.5±1.1	1.2
10	**41**[b]	27±3	52±11	1.9
11	**42**[c,e]	30.1±1.8	49±5	1.6
12	**49**[b]	8.5±0.3	5.53±0.11	0.6

[a] n.d. due to thermal instability during enzymatic assay. [b] 100 µM inhibitor concentration. [c] 50 µM inhibitor concentration. [d] 25 µM inhibitor concentration. [e] 1% DMSO present in assay buffer.

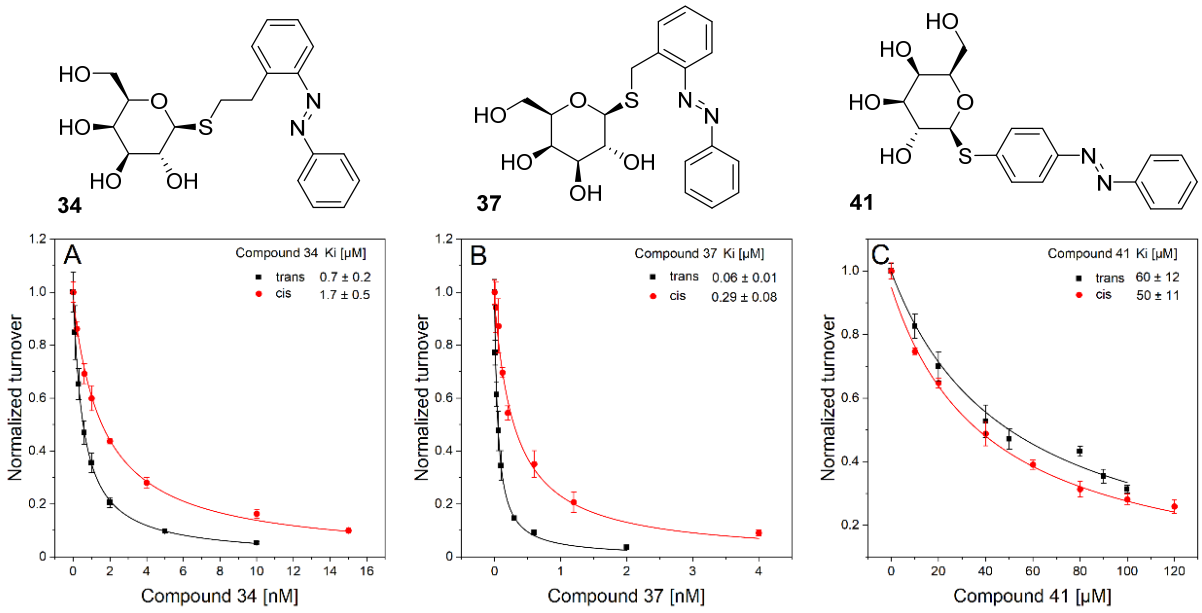

Figure S13. Normalized β-galactosidase kinetics at 100 µM substrate concentration at different concentrations of (A) compound **34**; (B) compound **37** and (C) compound **41** either in its *trans*-isomeric state (black lines; thermal equilibrium) or its *cis*-PSS (red lines). An enzyme concentration of 36 pM was present in all experiments. Error bars indicate the standard deviation of three independent measurements. Enzyme kinetics were additionally measured at 50 and 150 µM substrate concentration and the inhibition constant K_i was calculated as the average over these measurements.

References

1 A. G. Watts, T. Kantner, A. B. MacKenzie, *Assignee The University of Bath,* 2010, **WO2010070300A2**.
2 L. M. Doyle, S. O'Sullivan, C. Di Salvo, M. McKinney, P. McArdle, P. V. Murphy, *Org. Lett.,* 2017, **19**, 5802-5805.
3 H. Wang, S. Sun, J. Cheng, *Tetrahedron Letters,* 2017, **58**, 3875-3878.
4 L. Lindner, P. Klüfers, *Z. Anorg. Allg. Chem.,* 2015, **641**, 1869-1873.
5 M. P. Seed, H. J. Gutcke, *Assignee Diosamine Development Corporation Patent,* 2008, **WO2008059003 A1**.
6 R. Rajaganesh, A. Gopal, T. M. Das, A. Ajayaghosh, *Org. Lett.,* 2012, **14**, 748-751.
7 X. Xiao, Y. Zhao, P. Shu, X. Zhao, Y. Liu, J. Sun, Q. Zhang, J. Zeng, Q. Wan, *J. Am. Chem. Soc.,* 2016, **138**, 13402-13407.
8 X. Li, L. Huang, X. Hu, X. Huang, *Org. Biomol. Chem.,* 2009, **7**, 117-127.
9 M. Polakova, S. Sestak, E. Lattova, L. Petrus, J. Mucha, I. Tvaroska, J. Kona, *Eur. J. Med. Chem.,* 2011, **46** (3), 944-952.
10 D. Zhao, M. Johansson, J.-E. Bäckvall, *Eur. J. Org. Chem.,* 2007, **26**, 4431-4436.
11 N. Marquestaut, A. Martin, D. Talaga, L. Servant, S. Ravaine, S. Reculusa, D. M. Bassani, E. Gillies, F. Lagugné-Labarthet, *Langmuir,* 2008, **24**, 11313-11321.
12 M. J. Mickert, H. H. Gorris, *J. Phys. Chem. B,* 2018, **122**, 5809-5819.
13 O. Trott, A. J. Olson, *J. Comput. Chem.,* 2010, **31**, 455-461.
14 E. Krieger, G. Vriend, *Bioinformatics,* 2014, **30**, 2981-2982.